STUDIES TOWARD DEVELOPMENT OF UNIFIED MODEL FOR SOLID FRICTION FOR DENSE PHASE PNEUMATIC CONVEYING OF THE FINE POWDERS

A Thesis submitted
in partial fulfillment of the requirement for
the award of the degree of

Master of Engineering
In
Thermal Engineering

Submitted by

Amritpal Singh

Registration No.: 801583002

Under the supervision of

Dr. S.S. Mallick

(Associate professor MED)

DEPARTMENT OF MECHANICAL ENGINEERING

THAPAR UNIVERSITY, PATIALA-147004, PUNJAB, INDIA

June 2017

CERTIFICATE

I, Amritpal Singh, declare that the work presented in this thesis report entitled, **"Studies Toward Development of Unified Model for Solid Friction for Dense Phase Pneumatic Conveying of the Fine Powders"** is an authentic record of my work carried out as requirements for the award of the degree of **Master of Engineering** in **Thermal Engineering** at **Thapar University, Patiala** under the supervision of Dr. S.S. Mallick (Associate Professor, Department of Mechanical Engineering, Thapar University, Patiala) from July 2015 to June 2017. The matter presented in this thesis has not been submitted either in part or full to any other University or Institute for the award of any other degree.

Date: 26/6/17

Amritpal Singh

Amritpal Singh

It is certified that the above statement made by the student is correct to the best of my knowledge and belief.

(Dr. S.S. Mallick)
Associate Professor
Mechanical Engineering Department,
Thapar University, Patiala

Dedicated to

my parents

Acknowledgements

I would like to express my deep sense of gratitude and indebtedness to my supervisor, Dr. S.S. Mallick, Associate professor, Mechanical Engineering Department, Thapar University for their worthy guidance and encouragement. I am specially thankful to Mr. Atul Sharma, who guided me for experimental work and Dr. Anu Mittal for her support in my research work.

Finally I would like to express my very sincere gratitude to my parents for providing me with unfailing support and continuous encouragement throughout my years of study. This accomplishment would not have been possible without them. Thank you.

Amritpal Singh

Abstract

The dense phase mode of flow is widely used to convey different materials in various industries such as power, chemical, pharmaceutical, alumina, limestone, refineries, owing to its advantages such as lesser particle degradation, higher efficiency, smaller gas-solid separator, increased pipeline life as compared to dilute phase. The solids friction factor is an important factor to be included in empirical models to calculate the pressure drop. The available empirical models (grouping of different dimensionless term) for solids friction factor of fluidized dense phase flow are material specific, that is the values of constants and exponents are different for different materials. Even for the same material these constants vary due to difference in their particle size distribution. Therefore in the present study an attempt has been made to develop a unified model for solids friction factor. First, the most reliable two layer models for ESP dust, two types of fly ash, cement for short straight horizontal pipeline have been used for the derivation of unified constants with the help of dimensionless terms such as Froude number of particles, density ratio and particle size distribution. In order to validate the accuracy and stability of the unified two layer model, concept of equivalent length (to compensate the bend and vertical length loss) has been utilized to predict the total pipeline pressure drop in different pipeline (69 mm I.D. × 169m, 105mm I.D. × 169m, 65mm I.D. × 254m) and have been compared with experimental data. The results thus obtained provided the accurate prediction of pressure drop at lower as well as higher mass flow rate. But this correlation is valid for very small range of 'δ'. Due to this limitation, a new unified model was developed with three dimensionless terms by considering the wide range of data and then this model was validated with experimental data of Thapar University for grey and white cement which was conveyed in a 54mm I.D. × 70 m long pipeline. Also, the unified correlation has been defined to determine the pressure minimum curve with the inclusion of Stoke number and integral length scale of eddy for fine powders. This correlation has been validated with the experimental data of the given materials in different pipeline configurations. The correlation seems to predict the experimental data quite accurately.

Key words: Fluidized dense phase flow, Pressure minimum curve, and Solids friction factor.

Table of Contents

List of Figures

List of Tables

List of symbols and abbreviations

C	Particle velocity [m/s]
d_{50},d_p	Median particle diameter [μm]
D	Diamter of pipe [m]
Fr_p ,	Particle Froude number based on single particle terminal velocity and particle diameter ($Fr_p = w_{fo}/(gd)^{0.5}$)
Fr_g	Froude number with mean conveying velocity and pipe diamter
K, K_1	Constant of power function
L_e	Equivalent length (m)
L_h	Length of a horizontal portion of pipe [m]
L_v	Height of a vertical section of pipe [m]
l_e	Integral length scale of eddy [m]
m_f	Mass flow rate of air [kg/s]
N	Number of bends
Re_{sd}	Modified Reynolds number based on suspension density and particle diameter $\left(\frac{V_m \ d_{50}\rho_{sus}}{\eta}\right)$
St	Stoke number with inlet velocity $\left(\frac{V_i \ \rho_p \ dp^2}{18\mu D}\right)$
V	Superficial air/gas velocity [m/s]
V_i	Superficial velocity at inlet of pipe [m/s]
VLR	Volumetric loading Ratio ($VLR= (m_s/\rho_s)/(m_f/\rho_s)$)
w_{fo}	Single particle settling (or terminal) velocity in undisturbed fluid [m/s]
β_o	Velocity ratio related to particle fall velocity in a cloud ($\beta = w_{fo}/V$)
λ_a	Air/gas only friction factor
λ_s	Solids friction factor through straight pipe
λ_s*	Impact and friction factor
ρ_p	Particle density [kg/m^3]
ρ_b	Bulk density [kg/m^3]

Superscripts

a,b,c	Exponents of the power function

Abbreviations

I.D.	Internal diameter of pipe
PCC	Pneumatic conveying characteristics
PSD	Particle size distribution ($d_{50}/(d_{90}-d_{10})$)

CHAPTER 1

Introduction and Objectives

1.1 Introduction

The transportation of bulk solids from multiple sources to multiple destinations through pipelines with the help of gases is called pneumatic conveying. It has wide range of applications from the domestic vacuum cleaner to the transportation of products over several kilometers. Chemical process, pharmaceutical, agriculture, mining and mineral industries are the major industrial applications of pneumatic conveying systems. Either positive or negative pressure system are used to transport the materials. Generally the negative systems are used to transport materials for short distances because of the limitation due to vacuum pressure. Also materials which are hazardous to health are best transported by a negative system, while positive pressure systems are used for long distances. Air is commonly used as a carrier fluid and also some inert gases such as nitrogen, helium etc. are used to transport explosive and reactive products.

The transportation of products through pipeline can be categorized into two modes of flow i.e. dilute and dense phase flow. In the dilute phase flow, the velocity of carrier fluid is higher (and hence greater mass flow rate of fluid) to keep the particles in the pipeline suspended for conveying whereas, as the velocity of carrier fluid decreased, the flow of gas-solid mixture transitions from dilute to dense phase in the pipeline. Conventionally, the materials were transported in dilute phase flow owing to its benefits such as high reliability, greater tolerance and no blockage. However for dilute phase, the system requires higher velocity so a large size compressor is required. Also the size of air solids separator (i.e. bag filter) increases. Due to high particle velocity the life of pipeline decreases and quality of product also suffers as particles collide with pipe surface and other particles (i.e. product attrition increases) (Setia 2016). Due to these limitations of dilute phase, the low velocity dense phase flow is growing popular in various industries such as pharmaceutical, refinery, power, alumina, coal and ash.

The dense phase flow can be further classified into:

1). Plug/slug flow (particle diameter > 500 μm, loose poured bulk density (ρ_b) < 10^3 kg/m^3) and

2). Fluidized dense phase flow (particle diameter < 100 μm)

The granular products (particle diameter > 500 μm) and with small size distributions, convey as discrete plugs along the length of pipe with the plug diameter being approximately equal to that of the bore of pipe (Jones 1988). Whereas in the case of fine particles (particle diameter < 100 μm) with large size distribution, particles convey in a wave like motion at the bottom of pipeline constituting the fluidized dense phase flow. It makes both suspension and non-suspension layer, the majority of particles transport in the non-suspension layer. In plug/slug flow, the transition of granular products and small size distribution from dilute to dense phase or vice versa is unstable and severe pipeline vibration and large pressure fluctuations occur when that happens (Williams 2008). On the contrary, in fluidized dense phase flow the flow transition of fine particles from dilute to dense phase is very smooth which is attributed to the high air retention capability (Willam 2008). The advantage and disadvantages of pneumatic conveying system as mentioned below by Wypych (2006) are:

Advantages of pneumatic conveying system

a. Environment friendly transportation of a large variety of products.
b. Low maintenance and manpower costs.
c. Variety of products can be transported in a single pipeline.
d. Easy to automate and control pneumatic conveying systems.
e. Flexibility in routing is possible by the addition of bends.

Despite a lot of advantages the pneumatic conveying system has some disadvantages too.

a. High power consumption
b. Wear and abrasion of equipment
c. Limited conveying distances

Fine particles are mostly transported in the fluidized dense phase in the industry, because of the absence of unstable zone during flow transition from dilute phase to dense phase or vice versa. For

reliable conveying, the minimum velocity of carrier fluid and the total pipeline pressure drop are required. There is some understanding of what the effect of particle size, density and low loading ratio is, on the pneumatic conveying of bulk solids. However, that understanding is still not adequate as the flow in fluidized dense phase is highly turbulent and complex in nature (Mallick 2009). Due to this reason researchers (Stegmair,(1978); Pan and Wypych, (1998); Willam and Jones, (2004); Mallick and Wypych (2009); Mallick et al. (2013); Setia et al.,(2014), (2015), (2016)) preferred the power based empirical relations to predict the pipeline pressure drop instead of employing analytical methods. That is why, there are a number of empirical relations available to predict pressure drop for different materials but still there is the lack of a unified model. Some empirical relations are only applicable to the researchers own data. This thesis is an attempt toward the development of unified modelling of solids friction factor. Also, for optimization of conveying of fine powders, the modelling of pressure minimum curve has also been done.

Objective

- To carry out the experimental work for various products (grey/white cement) to determine total pipeline pressure drop (54 mm I.D. × 70 m).
- To develop a unified validated solids friction factor model to predict the pipeline pressure drop for dense phase flow.
- To develop a unified validated relation for pressure minimum curve

CHAPTER 2

Literature Review

2.1. Introduction

The author has reviewed different studies that have been conducted by various researchers over the years in this chapter. The literature includes various studies related to the different models of solid friction; effect of particle size, flow velocity, loading ratio and particle density on pressure drop and the components of pneumatic conveying system.

2.2. Components in pneumatic conveying system

A pneumatic conveying system can be divided into four distinct zones as mentioned by Klinzing et al. (2009). These are described as follows.

a) The Prime mover

Mass flow rate and pressure of air, which may be negative or positive are important to reliably and effectively convey materials. It can be achieved by a wide range of compressors, fans and blowers called prime movers.

b) Feeding, Mixing and Acceleration Zone

In this zone, material is fed into the pipeline and mixed with the flowing air stream, solids are accelerated from rest to the solid's conveying velocity. There are different type of feeding devices that can be installed such as rotary valve, venturi, screw and nozzle feeders.

Blow tank is used as a feeding device for high-pressure systems up to 500kPa (even more in some cases where it goes as high as 5000kPa, such as in coal gasification). The advantages offered by this feeding device are reduction of product degradation and erosion.

c) Conveying line

Once solid is accelerated, it enters the conveying zone which consists of bends, pipes, joints etc. The selection of conveying line material depends on the pressure drop and particle properties.

d) Separating zone

In this zone, conveying gas is separated from the particles with the help of cyclones or bag filters. Cyclones are gravity based so these are used for heavy particles and bag filters are used for fine powders (light weight particles). If material has a broad particle size distribution then both cyclones and bag filters are used and bag filters are arranged next to the cyclones.

2.3 Solids friction factors (λ_s)

It is an important parameter in predicting the pressure drop in fluidized dense phase pneumatic conveying. The correlations for dilute phase of solids friction factors (λ_s) have been well defined in the literature. Fluidized dense phase is more complex in nature, it is visualized in two layers, dilute phase layer on upper section and dense phase layer on bottom section of the pipe. Many researchers' correlations are defined below in table. Out of these correlations only one, Setia et al. (2016) proposed a two layer model of solids friction factor for fluidized dense phase.

Table 2.1: Different solid friction models

Author	**Models**
Stegmair (1978)	$\lambda_s = 2.1\ m^{*-0.3} Fr_m^{-2}\ Fr_s^{0.5}\ (D/d_s)^{0.1}$
Rizk (1982)	$\lambda_s = \lambda_s * C/V + 2\beta/\{(C/V)\ Fr^2\}$
Pan and Wypych (1998)	$\lambda_s = 3.2343\ (m^*)^{-0.47}\ (Fr_m)^{-1.56}\ (\rho_m)^{-0.43}$
Jones and Willams (2003)	$\lambda_s = 83/\{(m^*)^{0.9}\ Fr_i^2\}$
Willams and Jones (2004)	$\lambda_s = K(m^*)^a\ (Fr_m)^b$
Setia et al. (2015)	$\lambda_s = K\ (\frac{W_{f0}}{V})^a\ (VLR)^b$
Setia et al.(2016)	$\lambda_s = \tau_1 \left[(VLR)^a \left(\frac{W_{f0}}{V}\right)^b\right] \times \tau_2 \left[\lambda_s{}^* \frac{C}{V} + 2\beta_0/\{(C/V)\ Fr^2\}\right]$

In the above models, λ_s (solids friction factor) is the function of dimensionless terms such as Froude number, mass loading ratio, velocity ratio, density ratio, volumetric loading ratio, diametrical ratio. Inspection of these dimensionless parameters shows that there is need of justification in using some of these parameters in predicting the solids friction factor for fluidized dense phase conveying (Willam, 2008), namely:

$$\lambda_s = f(Fr_i, \frac{W_{f0}}{V}, m^*, VLR, \rho_m, D/d_s, Fr_m, Fr_s)$$

1. Froude number (Fr_i) shows the relationship of kinetic forces of conveying gas, with the gravitational forces and pipe diameter. Froude number is minimum for dense phase conveying.
2. Froude number (Fr_s) is the solid Froude number that shows the relationship between kinetic forces of particles and gravitational forces. It takes into consideration only single particle rather than bulk effect so it is same for dilute and dense flow.
3. Volumetric loading ratio (VLR) gives proportionality to the volume coupling between the volume of solids and conveying air. This term is effectively used in fluidized dense phase where pipe bore partially fills with the solids whereas remaining portion occupying by the conveying air.
4. Diametrical ratio (D/d_s) shows proportionality of particles to the pipeline. It describes the effect of particle size on flow properties during conveying of solid gas mixture with the diameter of pipe. Due to suspension of solids in dilute phase, this term significantly apply because the particle resistance behavior is dominated by dispersed particle events.
5. Dimensionless velocity ($\frac{C}{V}$) gives proportionality of particle velocity to the fluid velocity. The ratio of particle velocity to fluid velocity approaches to unity in dilute phase flow.

2.4 Previous research work

Barth (1958) proposed the expression for gas-solid mixture by considering separately pressure loss of air and solids through straight horizontal pipeline. This equation was employed by Weber (1981) for coarse particles in dilute phase flow.

$$\Delta P = \frac{(\lambda_a + m^* \lambda_s) L V^2 \rho}{2D} \quad (2.1)$$

All the parameters of this equation can be easily determined except for the solids friction factor. The phenomenon of gas-solid mixture flow mechanism is very complex to understand fundamentally so researchers used empirical approach by grouping different variables to determine the solids friction factor. Stegmair,(1978); Pan and Wypych, (1998); Willam and Jones, (2004); Mallick et al. (2013); Setia et al.,(2014), (2016) etc. used this expression to model solids friction factor for fluidized dense phase flow..

Stegmier (1978) was the first researcher who modeled the friction factor for solids by grouping four dimensionless parameters. The wide range of materials (mean diameter 15 to 110µm and particle density 1500 to 4100 kg/m^3) for both dilute and dense flow conditions in different size range of straight pipe have been used to develop this model as shown in equation(1). Weber (1981) modified the Stegmier (1978) solid friction model by replacing particle diameter in particle Froude number to pipe diameter as shown in equation (2.3).

$$\lambda_s = 2.1\ m^{*-0.3} Fr_m^{-2}\ Fr_s^{0.5}\ (D/d_s)^{0.1} \tag{2.2}$$

$$\lambda_s = 2.1\ m^{*-0.3} Fr_m^{-2}\ Fr_{sD}^{0.5}\ (D/d_s)^{0.1} \tag{2.3}$$

Rizk (1982) split the solids friction factor into two components in given equation (3), the first term (λ_s*) shows the impact and friction losses and second term ($2\beta/\{(C/V)\ Fr^2\}$) shows the losses due to particles kept in suspension, to determine the losses for dense phase flow. Wypych (1990,1990a) used $\beta_0\ (w_{fo}/V)$ instead of $\beta(w_f/V)$ to present this expression for dilute phase flow as shown in equation (4). Later, Setia (2016) developed a two layer model and used this expression for suspension layer.

$$\lambda_s = \lambda_s^* C/V + 2\beta/\{(C/V)\ Fr^2\} \tag{2.4}$$

$$\lambda_s = \lambda_s^* C/V + 2\ \beta_0/\{(C/V)\ Fr^2\} \tag{2.5}$$

Pan and Wypych (1998) developed the format of model in equation (2.6) by grouping three parameters). The values of constant are determined by considering the pressure difference of horizontal straight pipeline (between P9-P10) of fly ash and ESP materials with the “Regression” technique in the Data Analysis tool in MS Excel 2007. Eq. (6) and (7) are models of ESP dust and fly ash respectively. The dimensional mean air density term shows the variation of density in a pipe section.

$$\lambda_s = K_1 (m^*)^a (Fr_m)^b (\rho_m)^c \quad (2.6)$$

$$\lambda_s = 19.08(m^*)^{-0.88} (Fr_m)^{-2.39} (\rho_m)^{0.52} \quad (2.7)$$

$$\lambda_s = 14.5(m^*)^{-0.63} (Fr_m)^{-2.01} (\rho_m)^{-0.207} \quad (2.8)$$

Pan and Wypych (1998) conducted experiments of wide range of fly ash (particle density range 2197 to 2540 kg/m^3 and mean diameter range 4 to 58 μm) to obtain the single expression for fly ash. This expression is applicable to determining the losses in horizontal straight pipeline. Later, Setia (2014) evaluated this expression for our experimental data of fly ash and observed greater margin of error.

$$\lambda_s = 3.2343 (m^*)^{-0.47} (Fr_m)^{-1.56} (\rho_m)^{-0.43} \quad (2.9)$$

Jones and William (2003) provided the simple expression of a solids friction factor for fluidised dense phase flow with two dimensionless terms as shown in equation (2.10). The values of constants and exponents are determined by back calculation of four different materials such as pulverized fuel ash, iron powder, copper ore and flour (mean diameter range 42 to 90μm and particle density range 1470 to 5710 kg/m^3). In the back calculation, the losses due to bend, acceleration and vertical length are subtracted from total pipeline loss and hence expression is provided for only straight pipeline loss. It is the indirect approach to estimate the pressure drop of straight pipeline. In this calculation additional inaccuracy introduce in the accurate modelling because the limitation of accurate validated model of bend, acceleration and vertical length losses.

$$\lambda_s = 83(m^*)^{-0.9} (Fr_i)^{-2} \quad (2.10)$$

Datta and Ratnayaka (2007) considered that air and solid mixture is inseparable having its own flow properties and then determined pressure drop for both dilute and dense phase as modified by classical Darcy-Weisbach equation.

$$\Delta P = K \rho_{sus} L \frac{V_{entry}^2}{2D} \quad (2.11)$$

Barite (“mean particle size”:12μm), Bentonite (“mean particle size”:25 μm), cement (“mean particle size”:15.5 μm), ilmenite (“mean particle size”:9.5 μm), BC dry chemical powder (“mean particle size”:34 μm) and alumina (five different qualities of alumina with varied particle size distribution and mean particle size) were conveyed through six pipelines having different lengths

and diameters. Plots of K versus V_{entry}^2 were obtained. It was found that all the plots have similar trends and the pressure drop factor K is independent of pipe diameter and further, K for vertical conveying is independent of varied particle size distribution but Mallick (2009) wrote in his thesis that pressure drop factor K is dependent on pipe diameter because value of K may not be same for different diameters at a given mass flow rate of air.

Mallick and Wypych (2009) developed a criteria, based on Froude number for predicting minimum transport boundary by analyzing experimental data of different materials such as fly ash, ESP dust and cement to convey in different pipe lengths and diameters. Initially Froude number = 6 was proposed for safe design of conveying powder. but again, Setia and Mallick (2015) and Setia (2015) developed power based model in which Froude number is the function of mass loading ratio and the particle properties, for better prediction and safe design of pneumatic conveying powder.

Mallick et al.(2013) carried out experiments with fly ash (ρ_p :2300 kg/m^3, "median particle size":30 μm) and ESP dust ($\rho_{p:}$ 3637 kg/m^3; "median particle size":7 μm) and modelled the pressure drop factor,' K' for dense phase pneumatic conveying. The results showed that the suspension density and air velocity based models provide better prediction on scale-up than models based on conventional dimensionless term (Froude number and solid loading ratio).

Setia et al. (2014) proposed a simple correlation (eq. 2.12) of solids friction factor for fluidized dense phase conveying system. The author replaced conventional dimensionless term (Froude number and solid loading ratio) into volumetric loading ratio and superficial velocity. This model provided better prediction than the other models

$$\lambda_s = K\ (V)^a\ (VLR)^b \tag{2.12}$$

Later Setia (2015) replaced the superficial velocity by dimensionless velocity term (w_{fo}/V).

Recently Setia et al. (2016) developed a two layer model for fluidized dense phase pneumatic conveying system by transporting different materials such as fly ash, ESP dust and cement to determine solids friction factor.

$$\lambda_s = \tau_1 \left[(VLR)^a \left(\frac{W_{f0}}{V}\right)^b\right] \times \tau_2 \left[\lambda_s{}^* \frac{C}{V} + 2\beta_0/\{(C/V)\ Fr^2\}\right] \tag{2.13}$$

Second term of model was proposed by Rizk (1982), and modified (β to β_0) by Wypych (1990), for determining solids friction factor of dilute phase flow. The two layer model format better describes the fluidized dense phase flow behavior since both suspension and non-suspension region are taken into account. It predicts better on scale-up conditions than other models.

Behera et al. (2012) suggested a different approach to modelling fluidized dense phase conveying. The author used governing equations (continuity and momentum equations) to predict inlet flow parameters (pressure drop and mass flow rate of air) of pipeline. These equations are solved for single gas phase and certain number of solid phases (depend on particle size distributions). Initially author guessed the area factor (aa:"varies from 11 to 50") and friction coefficient (γ:" varies from 0.05 to 0.09") of solid phases. Experimental data of four different materials (two qualities of fly ash and two qualities of alumina) was used to compare predicted values and hence optimized area factor and friction coefficient for each material. The author used the minimum Froude number value for inlet boundary conditions given by Mallick and Wypych (2009), for reliable conveying. The results showed that friction coefficient varies linearly with the ratio of particle density to the mean particle size. Mills et al. (1982) and Arnold et al. (1986) proposed scaling specific correlations for air and solid mass flow rate that was used to analyse pressure drop of changed length and diameter.

Behera et al. (2013) did simulation by continuum approach in order to predict different flow parameters of dilute phase conveying through pipe. Governing equations (Continuity, momentum and energy equation) were solved with known exit boundary conditions by using MATLAB coding. Granular particle is assumed as granular gas, characterized by granular temperature and this parameter was included in energy equation. The results showed the variation of absolute pressure and granular temperature along the length of pipe for different values of tangential and normal restitution coefficients. But it is a challenge to choose optimum value of tangential and normal restitution coefficient for different materials and pipe surface.

Pan (1999) proposed a generalized flow mode diagram by using relationship between the loose poured bulk density and median particle size for bulk solid materials. The three different zones are depicted in the diagram, namely PC1, PC2 and PC3, these were obtained from experimental data and theoretical analysis of different products such as fly ash, agricultural catalyst, alumina, flour, granulated sugar, high silica flux, PVC powder, poly pellets, magnesium sulphate, mustard seed,

narasin, ply powder, iron powder, plastic pellets, pulverized fuel ash, potassium chloride, potassium sulphate, sugar, pulverized coal, pearlite, silica sand, slate dust WPP, wheat and zircon sand , barites, BPP, cement, coal, coarse sand copper ore, (particle diameters range from 11 to 4000 μm, particle density range from 800 to 4742 kg/m^3 and loose poured bulk density range from 100 to 2778 kg/m^3). If the material falls in the PC1 zone it can be smoothly transported in fluidized dense phase and dilute phase, the PC2 zone indicates that the material would be flow in dilute and slug phase, whereas, PC3 zone represents the dilute phase flow only.

Tong et al. (2016) predicted the dense phase pneumatic conveying behavior of granular and powder material by considering the effects of particle size distribution. They performed the experiments and analyzed the dense phase flow behavior of different materials such as lime (12 μm), fine CS ("median particle size":65 μm), mixed CS ("median particle size":240 μm), regular CS ("median particle size":400 μm), blue CS ("median particle size":600 μm) and magnesium ("median particle size":650 μm) having different particle size distributions pertaining to group A, group B and group D. The results showed that the materials below d_{50} < 70 μm, with a defined minimum air velocity, support fluidized dense phase flow and the materials that have narrow size distribution range d_{90}/d_{10} < 2.5 support low velocity slug flow and if the material does not satisfy the size and distribution range as mentioned above then it would prefer dilute phase flow.

Gore and Crowe (1988) explained the effect of particle size on augmentation or suppression of turbulence intensity, where they described that the turbulent energy of eddy is decayed by providing kinetic energy to smaller particles. On the contrary, larger particles increased the turbulence intensity due to the turbulence in its wake. The author has observed from various data of different material that the value of particle diameter to the integral length scale above 0.1, the turbulence intensity will increase and below 0.1 it will decrease.

Hetsroni (1989) conducted studies to account for the effect of particle Reynolds number on modulating the turbulent intensity, where they mentioned that the particles having Reynolds number more than 400 will increase the turbulence intensity due to vortex shedding in their wake, but particles with low Reynolds number suppress the turbulence through drag forces on the moving particle. The wide range of data, particle size (10-3000μm), from various researchers was verified.

Elgobashi and Trusdell (1993) conducted studies to investigate the effect of particles within the carrier fluid in modulation of the turbulent intensity, where they investigated several parameters

related to the phenomenon of “two way interaction” such as particle response time, particle diameter, volumetric fraction of solids and the effect of gravity. It was found that increasing the diameter of particles while keeping other properties same such as particle response time and volume fraction of solids, reduces the two- way coupling effect but the effect was more significant when the particle response time was doubled. The results also showed that in the absence of gravity, the decaying of homogeneous isotropic turbulence happens at a faster rate as compared to particle free turbulence but in the gravitational environment, the decay rate of energy reduces than in the particle free turbulence.

Lightstone et al. (2004) examined modulation of turbulence in the particle laden flow through pipe with the different models and developed a new model by accounting for the effect of crossing trajectories by particles. The results showed that the larger particles (i.e. the diameter of particles greater than 10% integral length scale) augmented the turbulent intensity and the models were able to predict the experimental data but could not include the production of turbulence due to the wake formation from larger particles.

Hadinoto et al. (2005) investigated the effect of fluid Reynolds number and particle size on gas-particle flow. Experimental work carried out with downward flow of two different size of spherical glass beads (70μm and 200 μm) at different gas-phase Reynolds number (in the range 6400 < Re <24000) and a constant particle loading (0.7). The results showed that the presence of smaller particle (70μm) dampens the turbulence up to the value of Reynolds number (8300) as compared to single phase flow, the enhancement of turbulence increases than single phase above Re >13800 but the turbulence in the larger particles (70μm) does not damp. They included the Stoke number to understand both, the responsive and unresponsive particles. The value of Stoke number is less than 1 for responsive particle, which follow the fluctuation of gas flow and governed by the fluid fluctuation equation, whereas, the value of Stoke number is greater than 1 for unresponsive particles, which do not follow the fluctuation due to its inertia.

Wang et al. (2006) conducted numerical studies to understand the response of particle in the fluid flow by different particle size (2, 20 and 200 μm). They also included the importance of Stoke number corresponding to the gas phase. These studies suggested that the particles follows the fluctuation of gas at low Stoke number (i.e. smaller diameter), whereas, the slip velocities increases

between two phases due to higher inertia for the larger particles. Thus the larger particles do not respond to the gas fluctuation.

Hidnoto et al. (2009) examined the effect of particle inertia, mass loading ratio on the modulation of turbulence, which is function of gas phase Reynolds number. The experimental results were obtained for two different loading ratio (0.4 and 4) and gas- phase Reynolds number (in the range of 6000 to 13000). For lower mass loading ratio (0.4), they observed the enhancement of turbulence for high particle inertia (St>500) and it increases with Reynolds number, whereas the presence of lower inertia particles (St<500) follow the fluctuation of gas. For the high mass loading ratio (4.0), the enhancement of turbulence for St>500, was not observed at higher Reynolds number, due to the increased magnitude of dissipative drag forces because of higher particles concentration.

The concluding points of these studies are listed below

1. To forecast the pressure drop, the two empirical approaches, first accounted for the contribution of gas and solids separately (Barth 1958 expression), whereas, second considered inseparable properties of gas – solid mixture (Datta and Ratnayaka 2007), and another analytical approach that includes governing equations have been discussed.
2. The physics of gas- solid interaction elaborated the modulation of turbulence, where the larger particles enhance the turbulence due to vortex shedding behind the particles, and smaller particles dampen the turbulence due to more dissipative forces than single phase flow. Some dimensionless parameters such as Stoke number, particle Reynolds number, gas-phase Reynolds number, and mass loading ratio are introduced to account for and create boundaries between augmentation and suppression of turbulence.
3. The observed results indicate that the gas and smaller particles interactions are inseparable, the smaller particles follow the gas fluctuation and dampen the turbulence, whereas, these results are obtained for very low mass loading ratio. For the higher range of m^* in the dense phase conveying, the effects of smaller particles on modulation of turbulence may be different due to the particle- particle collision, agglomeration of particles by cohesive forces such as Van der Waals, electrostatic and capillary forces. This indicates that the loading ratio of particles is also a considerable parameter to establish boundaries on augmentation and suppression of turbulence in pneumatic conveying of powders

CHAPTER 3

Experimental work and Development of pneumatic conveying characteristic

In this chapter, the test rig, instrumentation and product properties have been described.

3.1 Test facility in Thapar University and Experimental procedure

The test facility is available at Laboratory of particle and bulk solids in Thapar University to investigate the flow properties of gas-solids mixture. The following components have been installed to smoothly convey solids through pipeline in both dilute and dense phase.

- An electric powered screw compressor (Model: KES 18-7.5) is a prime air mover. It can supply the air at maximum pressure 700 kPa with 3.37 m^3/min. free air delivery. The moisture is removed from the air by refrigeration type dehumidifier. The dry air is stored in the air storage tank. It was installed to avoid the intermittent supply of pressurized conveying air. The capacity of air storage tank is 2m^3.
- 0.2 m^3 capacity bottom discharge blow tank with maximum permissible pressure 400kPa with solenoid operated dome type material outlet, inlet and vent valves have been installed. Receiver bin of capacity 0.65 m^3 have been mounted with the pulse jet bag filter on the top of blow tank.
- To record the pressure drop in the pipeline, the pressure transducer, manufacturer: Endress + Hauser ™, Current signal: 4-20mA, pressure range: 0-4 and 0-2 bar, model: Cerabar T PMC 131: have been installed in the different points on the pipeline as shown in the figure.
- Other instruments such as flow meter (12~24VDC flange connection vortex air flow meter), pressure reducing valve, non-return valve, flow control valve, on –off globe valve, load cells (shear beam type) were properly installed in the layout.

The flow properties of two fine powders such as grey cement and white cement were investigated. Both products were transported through 54mm × 70m pipeline at different mass flow rate of air and solid. The properties of products are described in the table 3.1. The particle size distribution was obtained using a laser diffraction analyzer (Malvern, Mastersizer 2000).

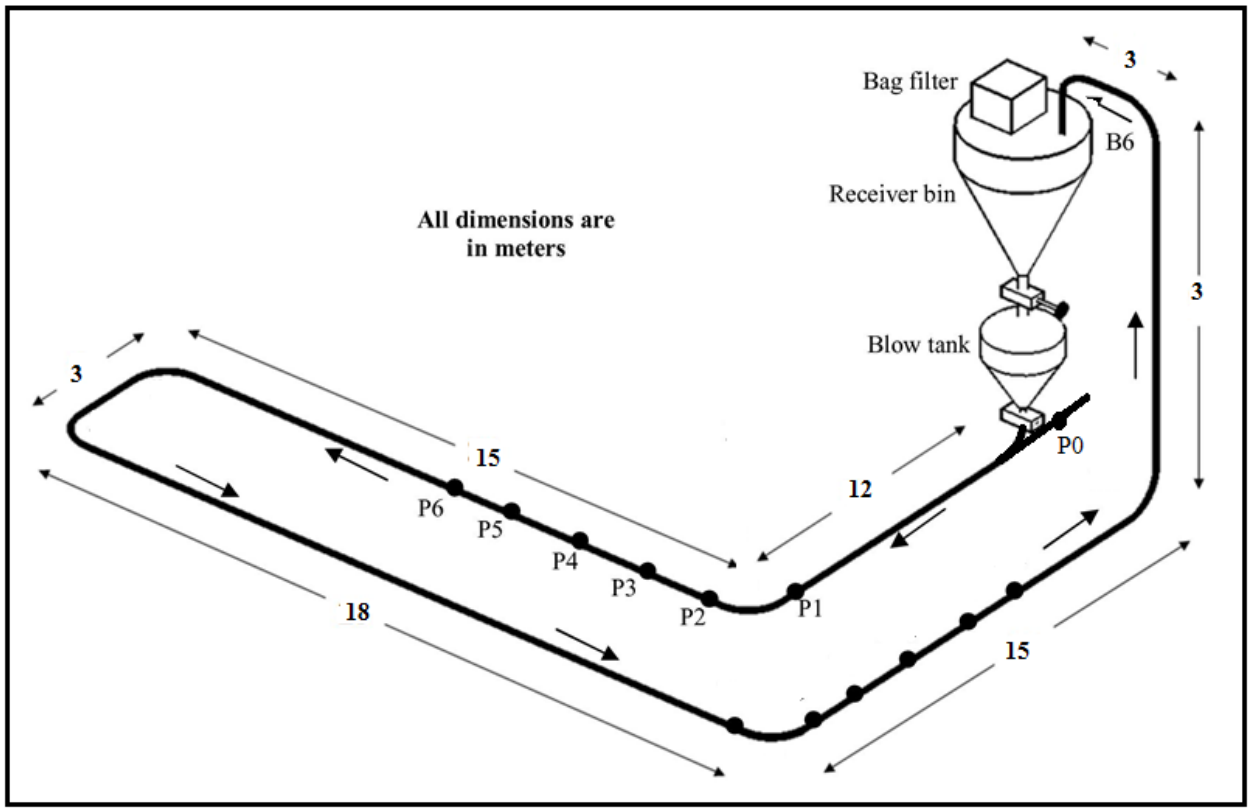

Figure 3.1. Layout of the 54 I.D. × 70m long pipeline test rig for both white and gray cement

Table 3.1. Properties of materials

Products	d_{10} (μm)	d_{50} (μm)	d_{90} (μm)	ρ_s (kg/m^3)	ρ_b (kg/m^3)
Grey cement	3	18	53	2680	1020
White cement	3	19	50	2720	1028

The various valves have mentioned in the figure 3.8 and a control panel was used for the operation. Amount of Inlet and outlet mass of solids in blow tank, pressurization & depressurization of blow tank was controlled by a control panel. The electrical output signal of pressure transducer, flow meter and data logger was recorded in a portable PC compatible data logger which consists of 16 different channel with 14 bit resolution. The recorded reading was stored in MS Excel in the PC.

3.1.1. Calibration of instruments and test procedure

The calibration of instruments is required to take actual readings. To obtain the actual readings, the calibration factor were determined before the experiment for load cell, flow meter and pressure transducer. The procedure of calibration of these instruments has been mentioned by Pan (1992). The following steps describes the calibration procedure of pressure transducer.

a.) The static pressure transducer were mounted at the desired place along the pipeline.
b.) The blind flange was used at the end of the conveying pipeline in order to cut the contact between pipeline and receiver bin.
c.) Build the pressure 100kPa inside pipeline by opening the globe valve, then leakage was checked. If there is leakage then static pressure suddenly drops.
d.) The manual pressure gauge was used to record the pressure inside the pipeline and simultaneously the pressure transducer recorded the pipeline pressure reading.
e.) The step (d) was used to record the different pressure readings by adjusting the pressure regulator.
f.) Then the Excel sheet was prepared with the different pressure transducer reading and manual pressure gauge reading and then make a plot to find the calibration factor. The total pipeline pressure transducer reading was plotted in the following graphs for both materials.

The load cell was calibrated by putting the known weight on the structure and simultaneously recorded the readings from data logger, then the graph was plotted between the different known values and data logger values. The digital vortex type flow meter displays the flow rate of conveying air. It was recorded by supplying the conveying air and simultaneously flow meter sent the analog signal to the data logger for recording digital reading. Hence it was calibrated.

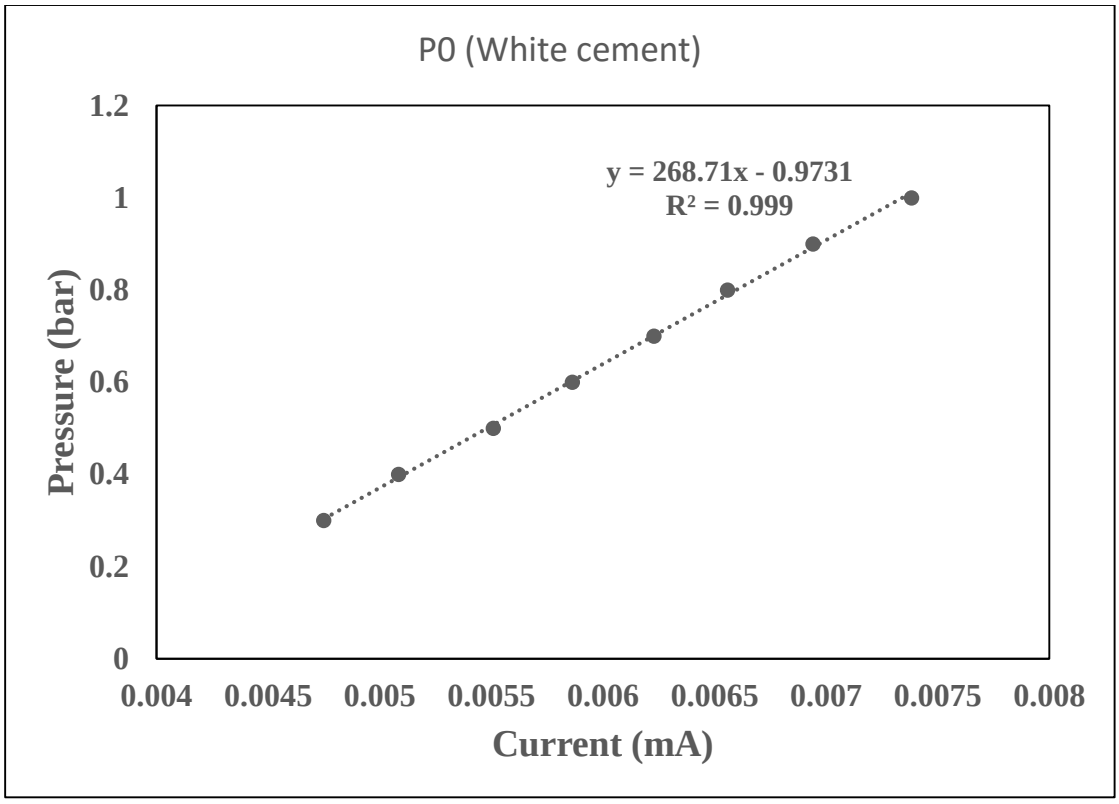

Figure 3.2 Calibration factor for P0 pressure transducer for white cement

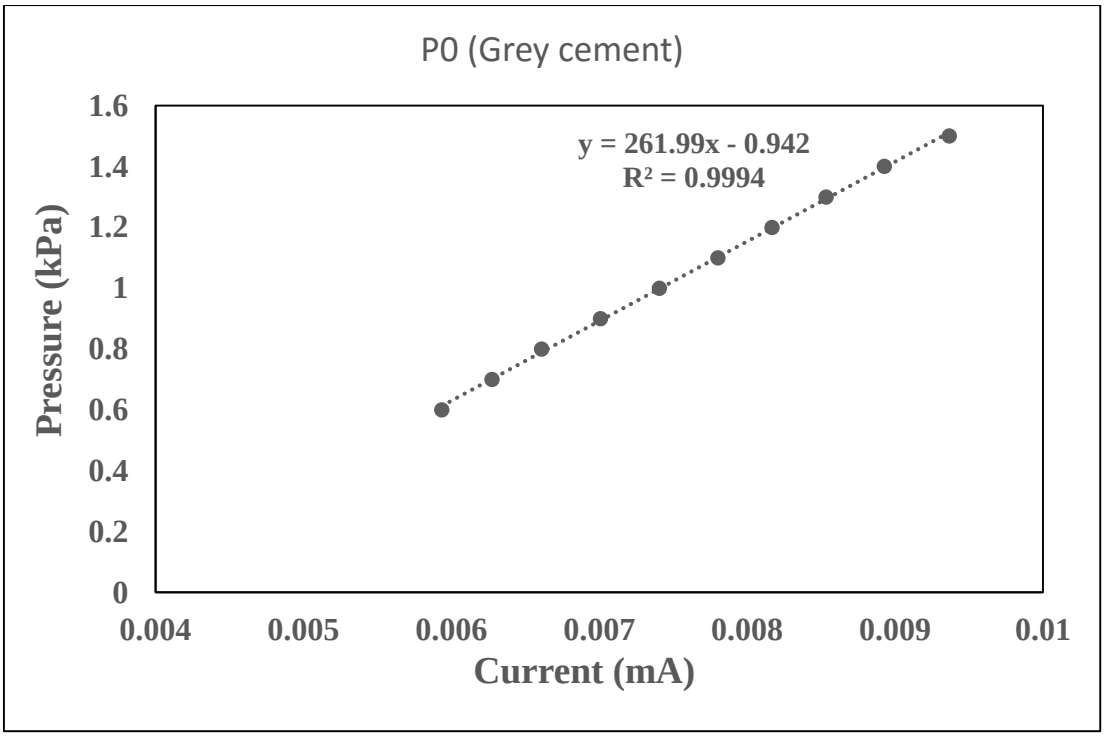

Figure 3.3. Calibration factor for P0 pressure transducer for white cement

In the literature, a standard procedure was mentioned to conduct experiments at different mass flow rate of solids and air (Wypych 1989, Mallick 2009). The figure (3.1) shows that the main air supply is divided into three parts, namely, fluidization air, top air and conveying air. Initially the flow rate valve for these three streams was fully opened. In the first batch of experiments, the conveying air valve opening was gradually decreased, however other two were fully opened. In the second batch of experiments, the top air valve was half closed while the conveying air valve was closed gradually from maximum to minimum. Some experiments were repeated to check the effect of product degradation on the experimental data.

3.2 Pneumatic conveying characteristic curve

The pneumatic conveying characteristic (PCC) curves are depicted between the pipeline pressure drops versus mass flow rate of air at different constant flow rate of solids. The analysis of PCC curves is important to obtain reliable conveying and optimized design of pneumatic transportation system. The steady state conveying curves provide valuable information such as optimum design (i.e. the pressure minimum curve), blockage conditions (minimum velocity for different products), pressure drop at particular mass flow rate of solids, and the flow properties (Pressure, velocity) of two products can be compared. To plot the PCC curves, the experimental data of load cell, pressure transducer and flow meter were recorded for each experiment in the MS Excel Sheet. The graph was plotted for pressure transducer points, flow meter reading and load cell with time to obtain the steady state conveying points. The conveying points at different mass flow rate of solids and air were obtained for both white cement and grey cement in the following figures.

The experimental data is unable to provide direct essential information regarding pneumatic conveying systems. Because, during experiments, the solids discharge rate is set to a constant flow, but, it vary to some extent for every experiment. So the PCC (pneumatic conveying characteristic) curves at constant solids rate were drawn to extract valuable information for particular product. The interpolation method was used to obtain constant solid lines from the different solids flow rate of experimental data. The procedure to select the two points for interpolation had been explained by Mallick (2009).

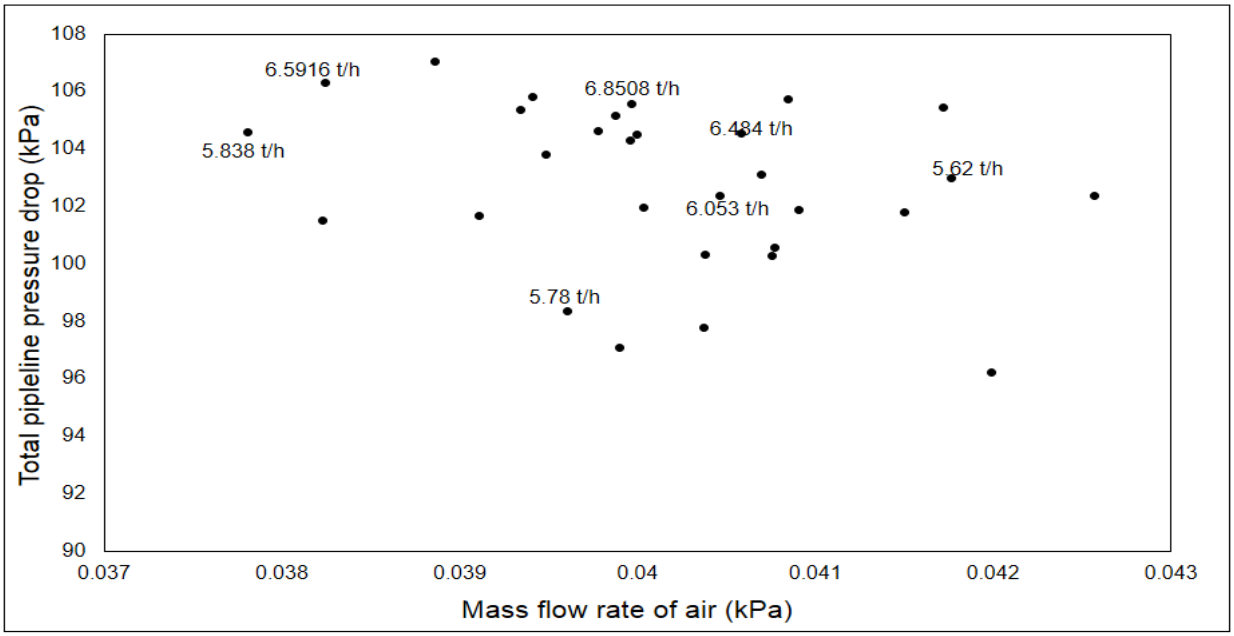

Figure 3.4. Experimental data points for total pipeline pressure drop versus mass flow rate of air for gray cement, through pipeline B4 (54 mm I.D. × 70 m long pipe)

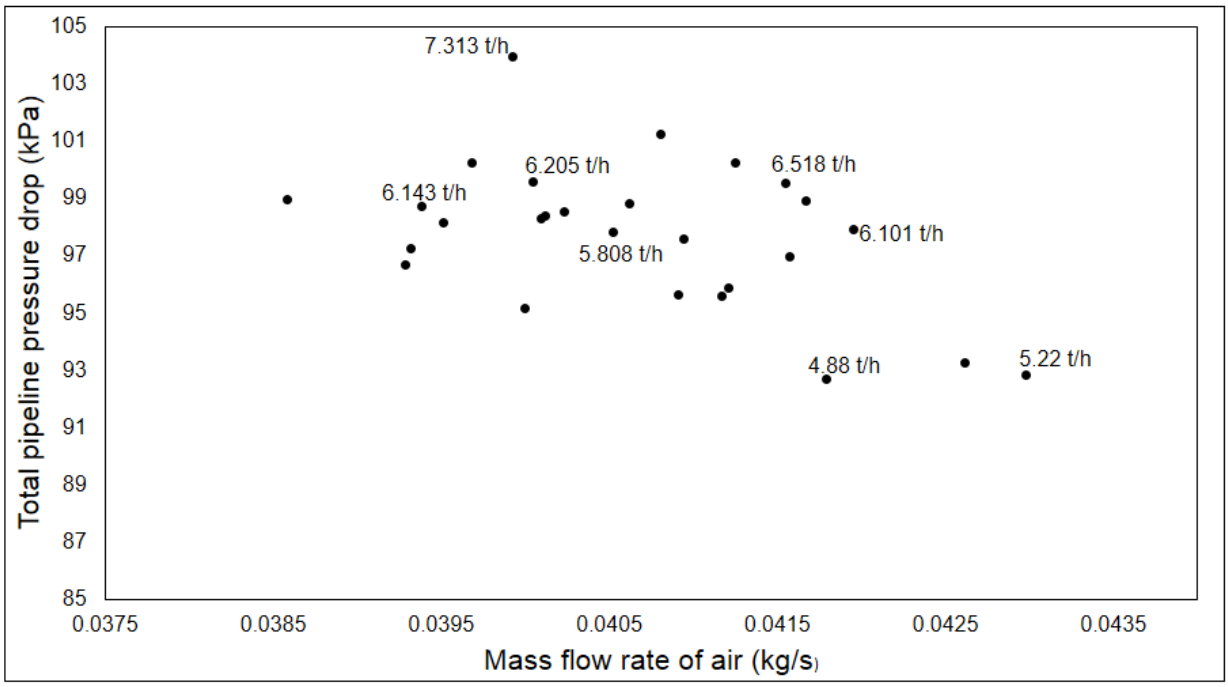

Figure 3.5. Experimental data points for total pipeline pressure drop versus mass flow rate of air, through pipeline (54 mm I.D. × 70 m long pipe.

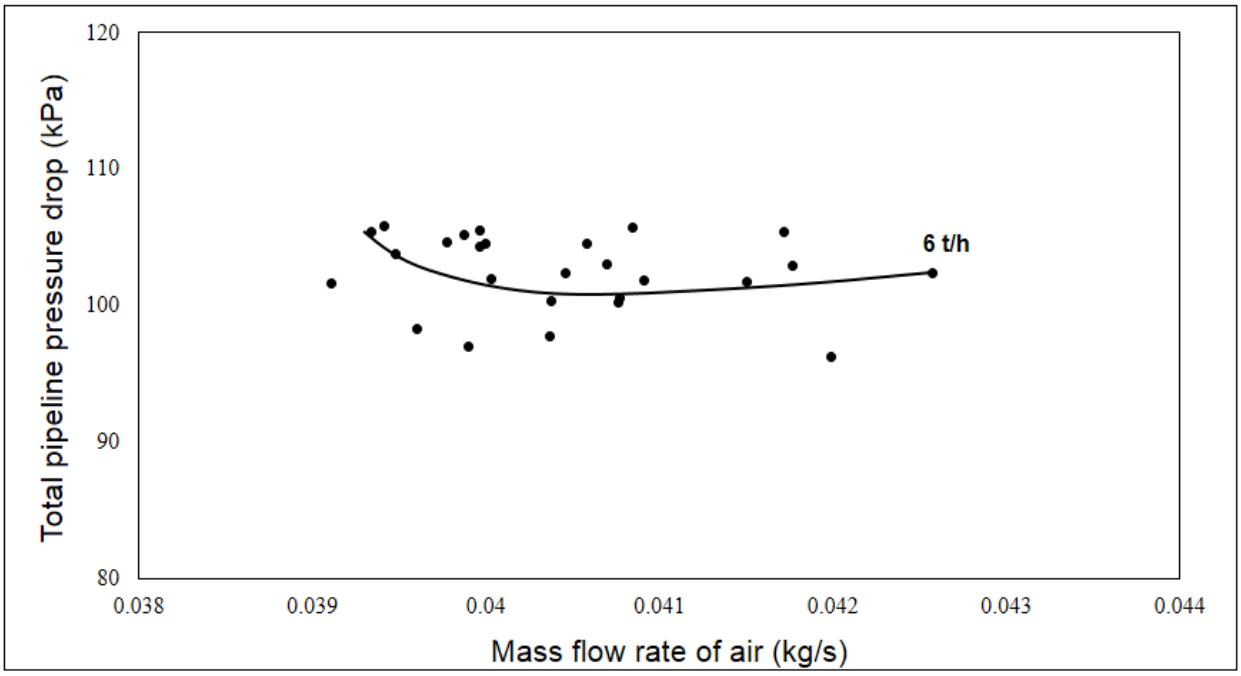

Figure 3.6: Total pipeline PCC for grey cement at 6 t/h of mass flow rate of solid, through pipeline (54 mm I.D. × 70 m long pipe)

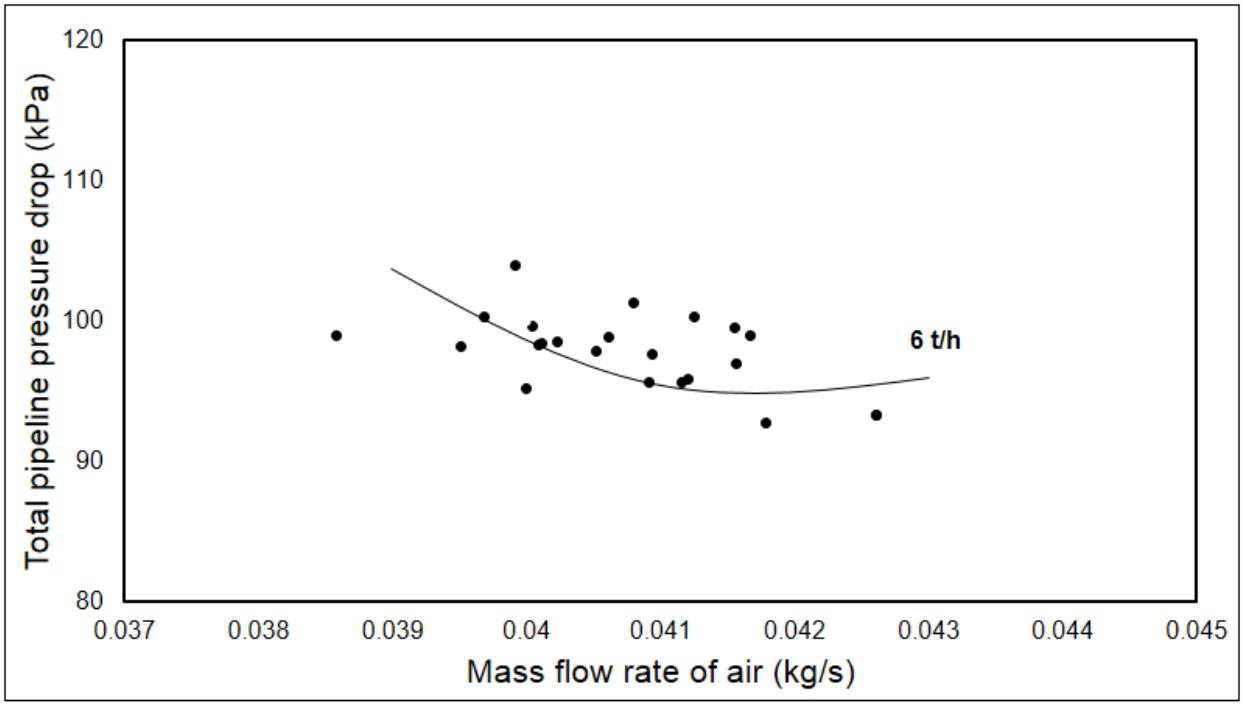

Figure 3.7: Total pipeline PCC for white cement at 6 t/h of mass flow rate of solid, through pipeline (54 mm I.D. × 70m long pipe)

The white cement and gray cement both were transported through pipeline 54 mm I.D. × 70 m long pipe and P0 pressure tapping recorded the total pipeline pressure drop. The total pipeline pressure drop includes the vertical and straight horizontal lengths, bends and initial acceleration losses. By the interpolation method, the final pneumatic conveying characteristic (PCC) curve in figure 3.6 and 3.7 is obtained for gray cement and white cement respectively at constant mass flow rate of solid from the experimental data of different mass flow rate of solid. The scatter points near the PCC curve (see in figure 3.6 and 3.7) are due to variation of different mass flow rates of solids from a constant solids line. The curve of PCC in both product smoothly transitions from dense to dilute phase as it is described in the literature for fine powders. The experimental data of both products were used to validate the newly developed unified model in chapter (4).

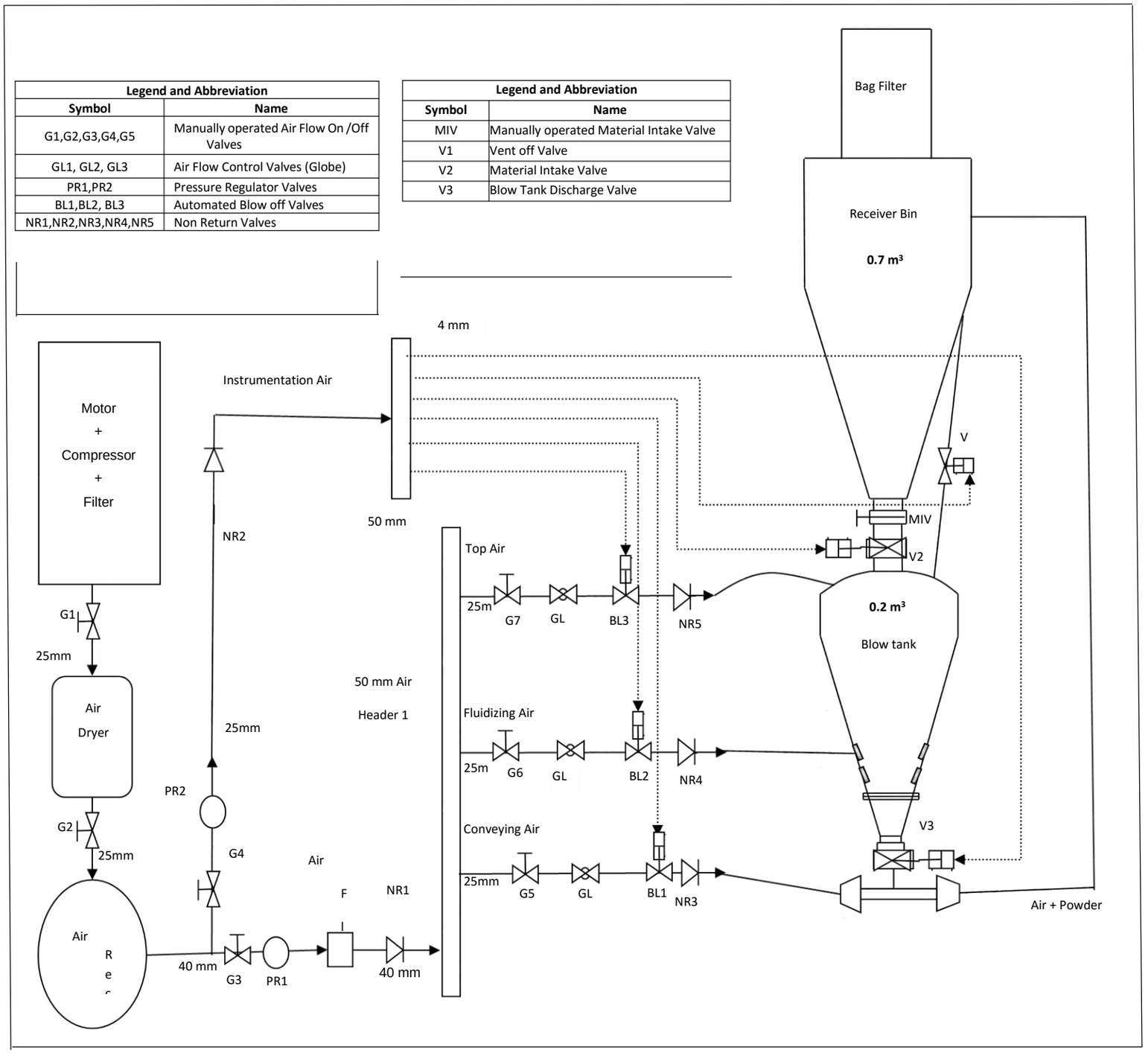

Figure.3.8: Schematic diagram of operation distribute and control the compress air supply from the dryer to conveying line, through blow tank

Chapter 4

Unified modelling and Scale up validation of solids friction factor

4.1. Modified two layer solid friction model

During fluidised dense phase conveying of fine powders most of the product is conveyed along bottom of the pipeline and some of the products flows in the suspension on top of this layer. The maximum portion of pipe bore is covered with non-suspension layer hence large amount of material is conveyed in the dense phase form and dilute phase layer flows over the non-suspended layer. Recently, the two layer model format (equation 2.13) was proposed by Setia (2016).The first term $\tau_1 \left[K(VLR)^a \left(\frac{W_{f0}}{V}\right)^b\right]$, which is the grouping of volumetric loading ratio and dimensionless velocity (ratio of terminal velocity to mean superficial velocity) addressed the modelling of dense phase layer and the second term $\tau_2 \left[\lambda_s{}^* \frac{C}{V} + 2\beta_0 / \left\{(C/V)\, Fr^2\right\}\right]$, which is Weber –A4 model has been considered for the suspension layer. τ_1 and τ_2 represents the relative contribution of dense phase and dilute phase layers.

The values of K, a, b and $\lambda_s{}^*$ are different for different materials, even the properties of same material could be different depending on the size distribution of the sample. The values of constants for specific materials are given in the table 4.1. In the literature, the effect of particle size distribution was not considered to model the solids friction factor, however it has been clearly observed that larger particles enhanced the turbulences due to vortex shedding in its wake, whereas smaller particles dampen the turbulent kinetic energy through drag forces (Grore and Crowe (1987). Geldart diagram shows that the fluidization behavior of material depends on the particle density and particle size, hence the gas-particle interaction properties such as fluidization, de-aeration and permeability vary with size distribution of particles. Later Tong et al. (2016) considered the effect of particle size distribution to predict the mode of flow. The results showed that the materials below d50 < 70 μm, support fluidized dense phase flow and the materials that have narrow size distribution range d90/d10 < 2.5 support low velocity slug flow and if the material

does not satisfy the size and distribution range as mentioned above then it would prefer dilute phase flow. Therefore literature suggests that consideration of particle size distribution is important to study the flow phenomenon. The exponent of dimensionless velocity 'b' is linearly varying with the particle size distribution as shown in the figure 4.2. Hence it shows that the contribution of terminal velocity of particle to predict solids friction factor varies with particle size distribution even when the materials are same. The exponent of volumetric loading ratio 'a' is depending on delta ('δ') that represents both dimensionless terms, particle size distribution and density ratio (ratio of bulk density and particle density) in given equation 4.1. The ratio of bulk density to the particle density represents the interstitial voids within the bulk materials, and the movement of gases in the voids represent the energy drop, so the contribution of volumetric loading ratio (the actually available portion of pipe for air flow by Setia (2016) has been decided with the density ratio and particle size distribution. The relation between 'a' and 'δ' is shown in the figure 4.1. Froude number of particle is the dimensionless term defined by terminal velocity and particle diameter has been opted in the place of constant 'K', it shows that the variation of constant 'K' depends on the single particle behavior and their properties rather than bulk behavior and $\lambda_s{}^*$ (the impact and friction coefficient) is replaced by terminal velocity of particle which is accounted by equating drag and buoyancy forces with the gravitational force (Klinzing 2011).

The constants of two layer model format was determined for only four materials by considering the pressure drop of straight horizontal short pipeline. It is the reason only four points are available for defining the relationship of constants with the particle and bulk properties.

Table 4.1: Values of constants of two layer solid friction for different materials (Setia (2016))

Products	K	a	B	w_{fo}	$\lambda_s{}^*$
ESP dust	2961	-0.21	1.73	0.005	0.0135
FA1	7.94	-0.26	1.51	0.06	0.0043
Cement	11.02	-0.37	1.44	0.036	0.0081
FA2	14.5	-0.54	1.59	0.038	0.0074

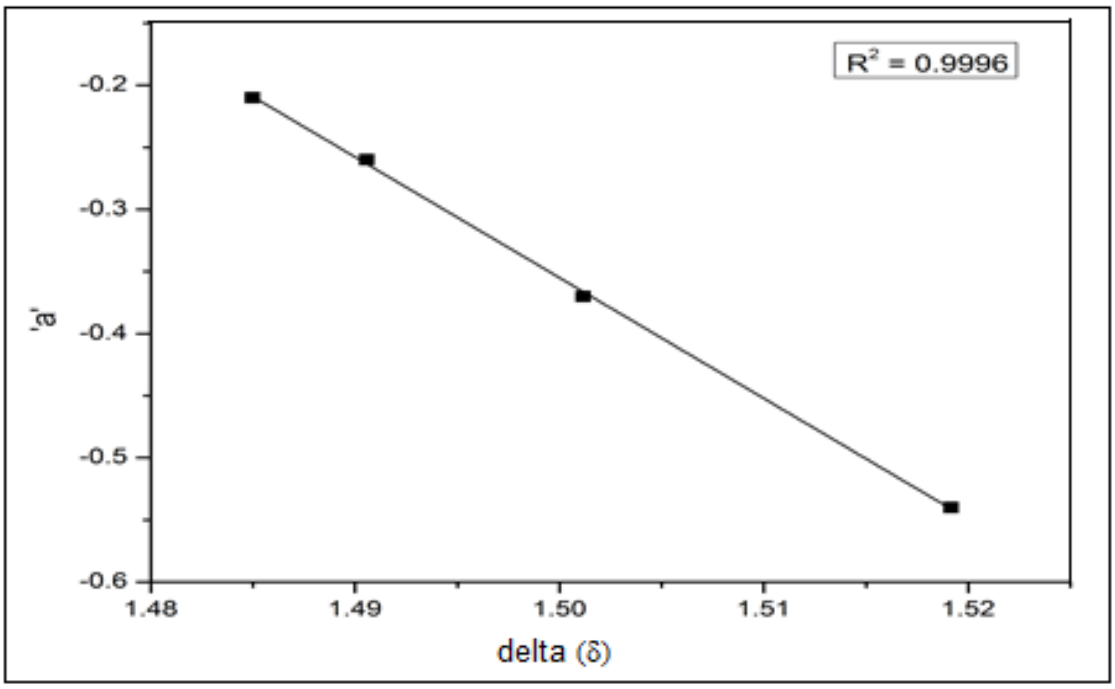

Figure 4.1: Variation of constant ‘a’with delta (δ)

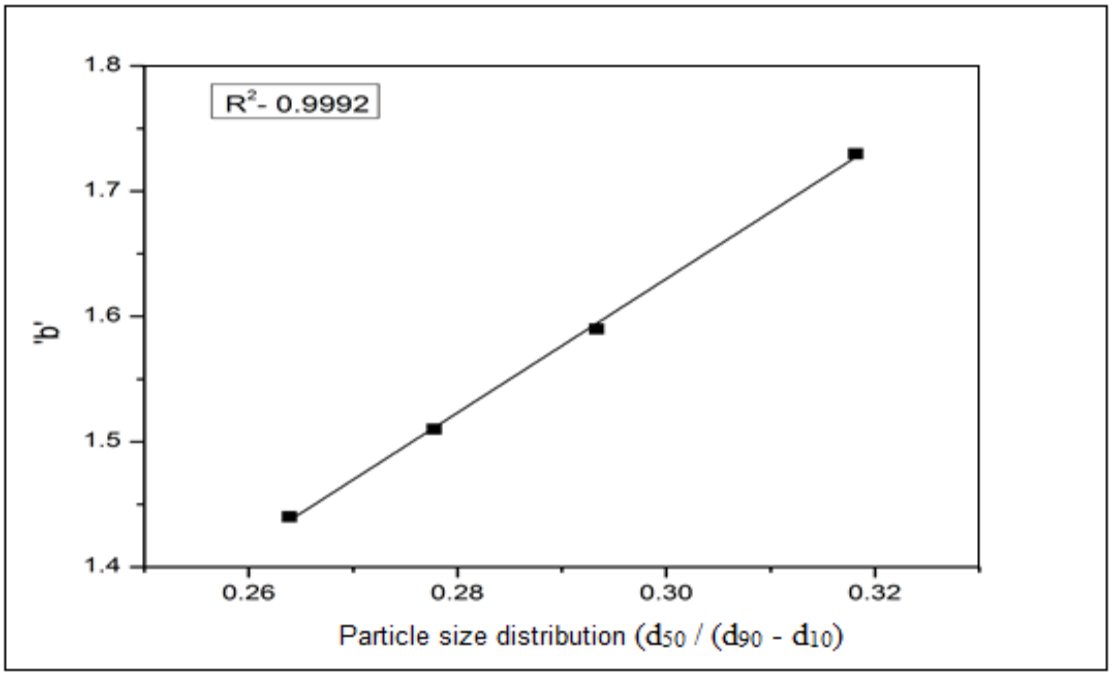

Figure 4.2.Variation of constant ‘b’ with the PSD (particle size distribution)

$$\delta = 3.38 \times (PSD) + (\rho_b / \rho_s)^{0.5} \quad (4.1)$$

$$\ln(K) = K_1 \, Fr_p^{(c)} \quad (4.2)$$

$$\ln(K) = 5.3866 \, Frp^{(-0.776)} \qquad R^2 - 0.9958 \quad (4.3)$$

$$\lambda_s^* = -0.1687 \, w_{fo} + 0.0142 \qquad R^2 - 0.995 \quad (4.4)$$

4.1.1. Scale – up validation

The data of following materials were used for scaling -up in the present study.

a) Fly ash (FA1) (Wypych et al., 2005)
b) ESP dust (Wypych et al., 2005)
c) Cement (Setia, 2014)
d) Fly ash (FA2) (Setia, 2014)
e) Fly ash (FA3) (Pan, 1992)

FA1 (Australian power station fly ash) and ESP dust were conveyed in the University of Wollongong at the Bulk materials Handling Laboratory , Australia by varying mass flow rate of air in different pipelines. The schematic diagram of University of Wollongong test rig (for one pipeline) is shown in the figure A1. The internal diameter is 69mm and length of pipeline is 169m with five 90° bends having 1m radius of curvature each and 7m of vertical length. The pressure transducers were employed along the pipeline on pressure tapings (P8, P9, P10, P11 and P12) to measure the pressure loss with the help of data logger system which was connected to a portable PC.

Schematics test rig of Fujian Longking Co. Ltd was used to convey FA2 (China fly ash) and Cement by varying mass flow rate of air is shown in the figure A2. The static pressure tapings (P1, P2 and P3) were employed along the pipeline to measure pressure loss. P1 was used to calculate total pipeline pressure drop.

The geometric configuration of pipelines and particle properties of all materials are shown in the table 4.3.

ESP dust

The unified two layer model was evaluated for larger diameter and longer pipe length to predict the solids friction factor in order to check the accuracy and stability the model by comparing with the experimental data. In the literature, previous researchers measured the straight, bend and vertical losses separately to determine the pressure drop across total pipeline and also different models for straight horizontal length, bend and vertical length were used for determining pressure drop for different materials. In this study, the bend and vertical length losses were compensated with the concept of equivalent length (discussed in section 4.2.2) and unified model has been validated by given products. The equivalent length of total pipeline is horizontal length, added to twice the vertical length plus four times the number of bends.

$L_e = L_h + 2L_v + 4N$

The ESP dust was scaled-up on different size ranges of pipe (I.D.69mm ×169m, I.D.69mm ×554m, I.D.105 mm ×169 m). The pneumatic conveying characteristic curves are used to compare the predicted values of larger and longer pipeline with the experimental data. The results of unified two layer model and concept of equivalent length for ESP dust are shown in the figure 4.3-4.5. The pneumatic conveying characteristic curves are obtained on different mass flow rate of solids.

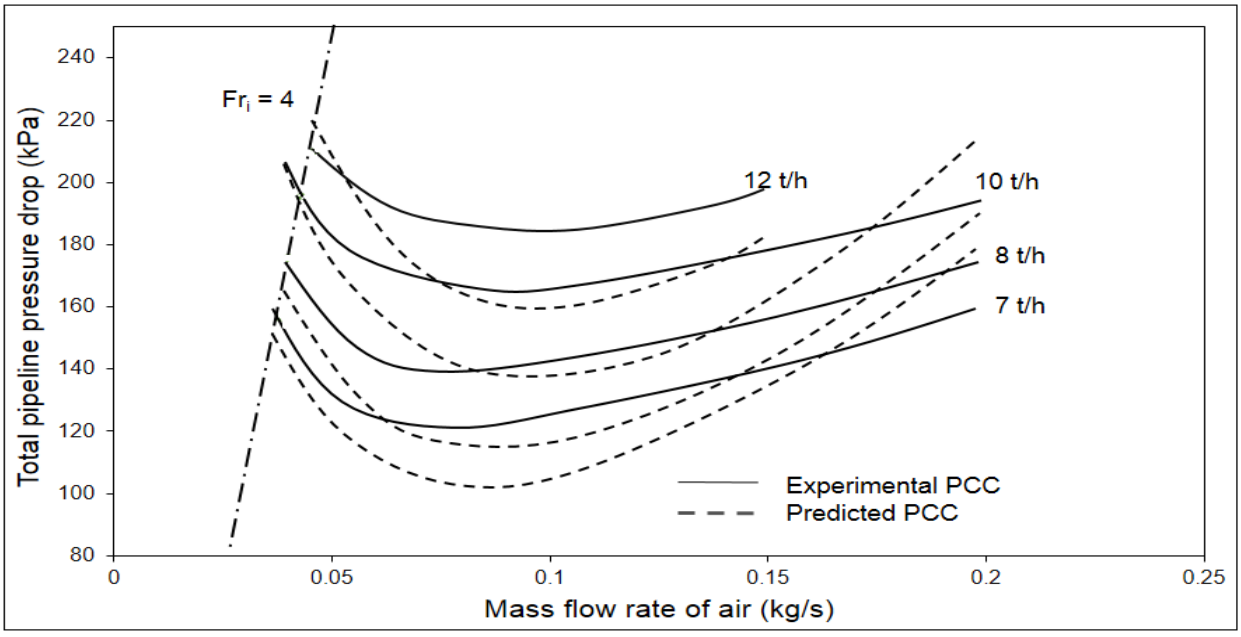

Figure 4.3. Experimental versus predicted PCC curve using unified two layer model and concept of equivalent length, ESP dust through 69 mm I.D. ×168 m long pipe.

Figure 4.3 shows that the experimental minimum transport boundary of ESP dust was at inlet Froude number 4. The results show reasonable accuracy at extreme dense phase while, increasing mass flow rate of air leads to under prediction. The trend of predicted PCC curves is U- shaped, same as experimental PCC curve. But the curves of predicted pressure drop are narrow while experimental PCC curves are broad. It means that the pressure drop has gradually changed by increasing mass flow rate of air in experiment. Possible reasons of under prediction could be because of high bend pressure and contribution of non –suspension term may be varying for this material.

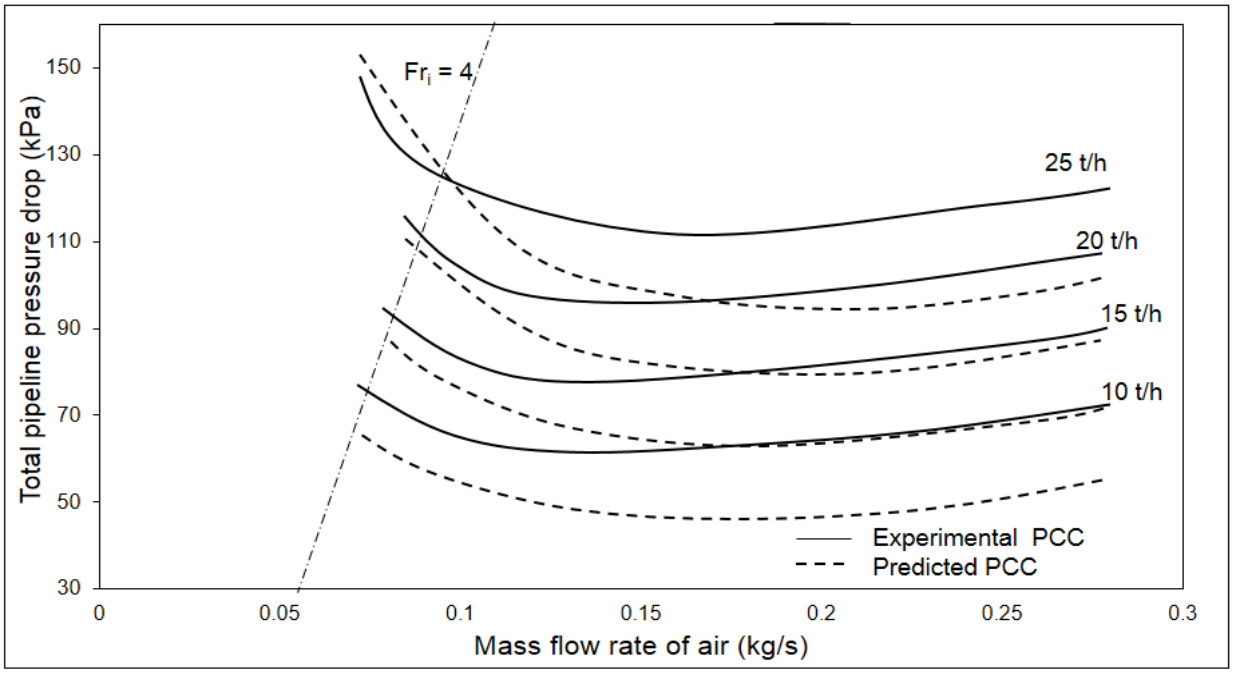

Figure 4.4. Experimental versus predicted PCC curve using unified two layer model and concept of equivalent length, ESP dust through 105 mm I.D. ×168 m long pipe.

Figure 4.4 shows the diameter scale –up of ESP dust with minimum transport boundary at Froude number 4. The trend of both predicted and experimental PCC curves is same. However, predicted PCC curves suddenly decreases near low Froude number and then remain same along increasing mass flow rate of air. The results are calculated well with slight under prediction before pressure minimum points but the error of under prediction increases with increasing mass flow rate of air. Surprisingly, in longer pipeline for this material (see figure 4.5) is over prediction. The percentage of over prediction is higher near the minimum Froude number = 3 whereas, in this case the

deviation by over prediction decreases with increasing mass flow rate of air. The trend of predicted and experimental PCC curves beyond the pressure minimum curve along the increasing mass flow rate of air is same. While, deviation toward decreasing mass flow rate is increasing. The higher over prediction at dense phase region attributed to the more number of bends at different location along the line.

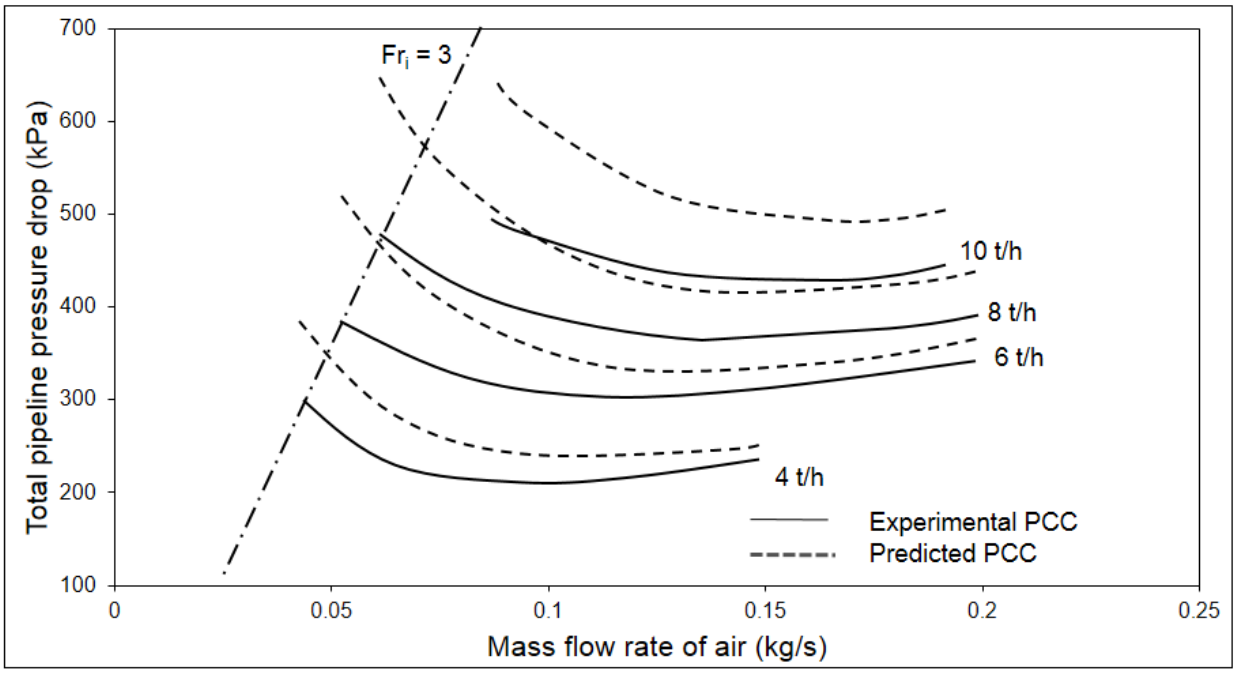

Figure 4.5: Experimental versus predicted PCC curve using unified two layer model and concept of equivalent length, ESP dust through 69 mm I.D. ×554 m long pipe.

Fly ash

Using the similar concept of ESP, the two different samples of fly ash were scaled up. FA1 and FA2 are two different fly ash samples and transported through different pipe diameter and length, results are shown in figure 4.6-4.9.

Results show that FA1 was transported at inlet Froude number 4 for shorter and larger pipeline (see in figure 4.6 and 4.8) and the trend of PCC curves in both pipeline is similar. Figure 4.6 and 4.8 describe reasonable well prediction at low mass flow rate of air up to pressure minimum point for each constant mass flow rate of solids. Error of under prediction substantially increases beyond minimum pressure drop. As the mass flow rate of air increases, inlet Froude number also grows simultaneously hence, the contribution of suspension term in two layer model is hiked. While for

this material the suspension term could not predict pressure drop well. Also, the bend loss increases with escalating the inlet velocity. It may be possible the equivalent length of 4 meter as per bend could be much higher for this material in dilute flow.

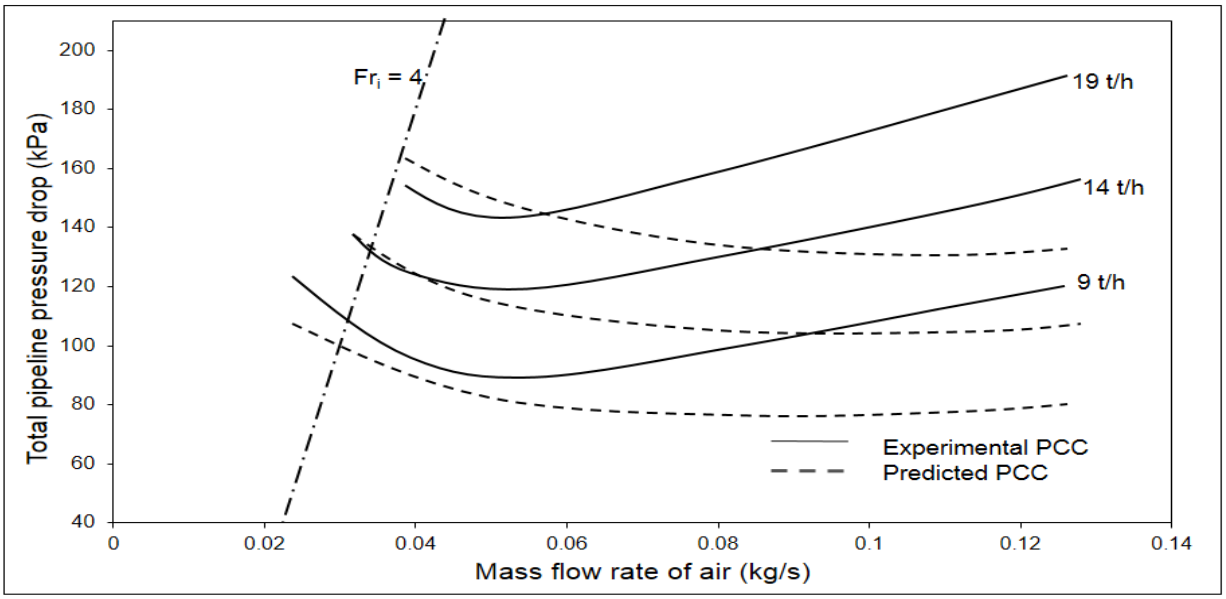

Figure 4.6. Experimental versus predicted PCC curve using unified two layer model and concept of equivalent length, FA1 through 69 mm I.D. × 168 m long pipe.

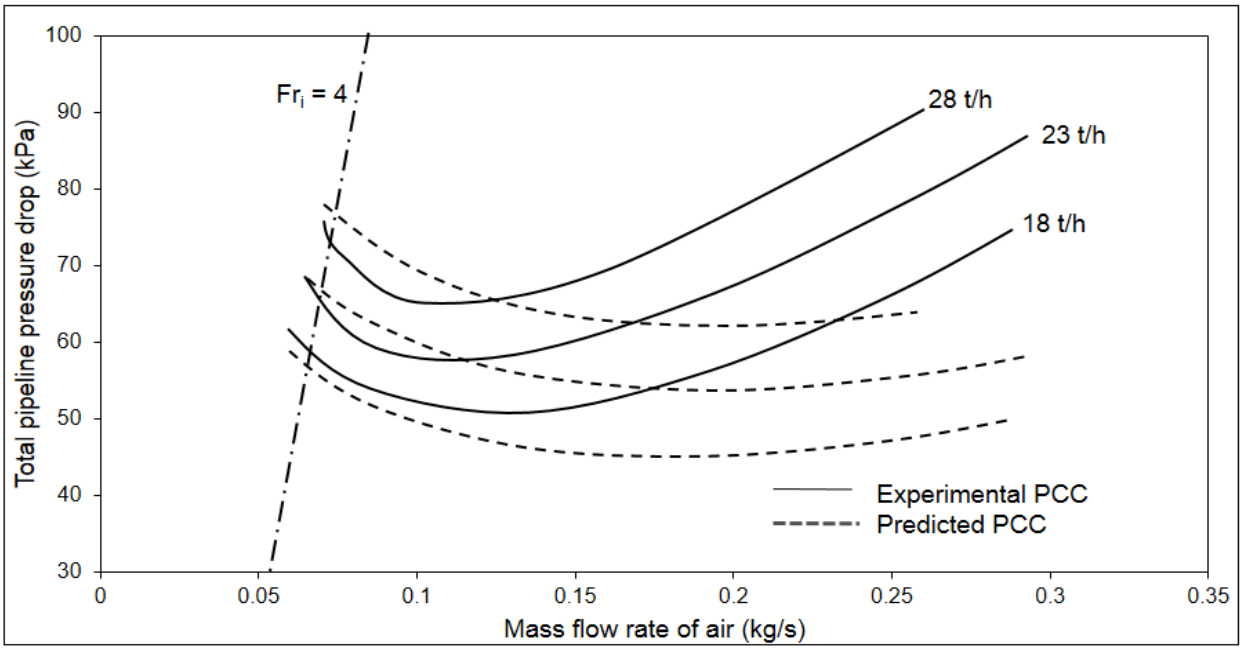

Figure 4.7. Experimental versus predicted PCC curve using unified two layer model and concept of equivalent length, FA1 through 105 mm I.D. ×168 m long pipe.

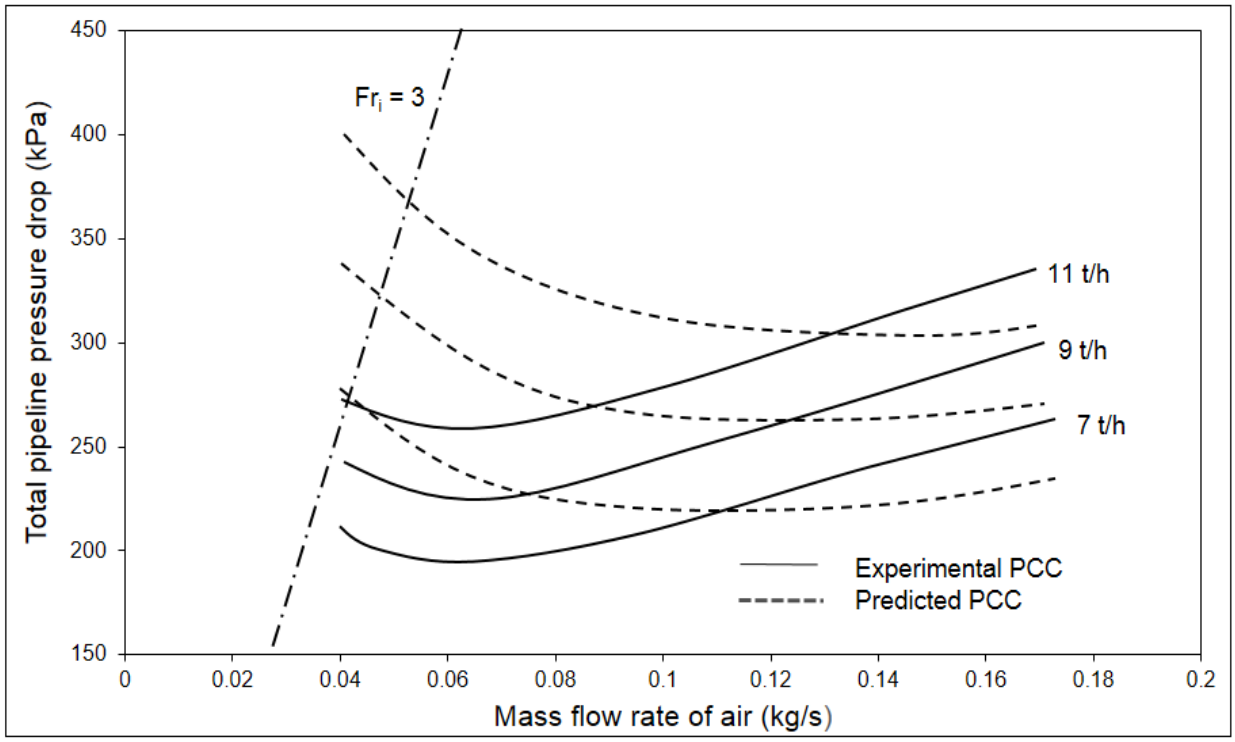

Figure 4.8. Experimental versus predicted PCC curve using unified two layer model and concept of equivalent length, FA1 through 69 mm I.D. × 554 m long pipe.

Interestingly, results for the FA1 in length scale up gives over prediction at dense phase (see in figure 4.8). Figure 4.8 shows that the minimum transport boundary for longer pipeline at Froude number 3. The slope of experimental PCC curves sharply increases and hence, at higher mass flow rate of air the results are showing under prediction. There could be possible reason of over prediction and under prediction are that the more number of bends at different locations along pipeline. As the velocity of air escalates along the length of pipe, the pressure drop around the bend at its different location would be different and for low mass flow rate of air the pressure drop around the bend may be less than as assumed in equivalent length while for higher mass flow rate of air it could be more than as considered.

Fly ash (FA2) was transported into the 65 mm internal diameter and 254 m long pipeline. Figure 4.9 shows that the Fly ash (FA2) is transported at minimum inlet Froude number 4.4. Results show that the trend of experimental and predicted PCC curves is same while, it is some under predicted for both higher and lower mass flow rate of air. Here is also under prediction attributes to the equivalent lengths.

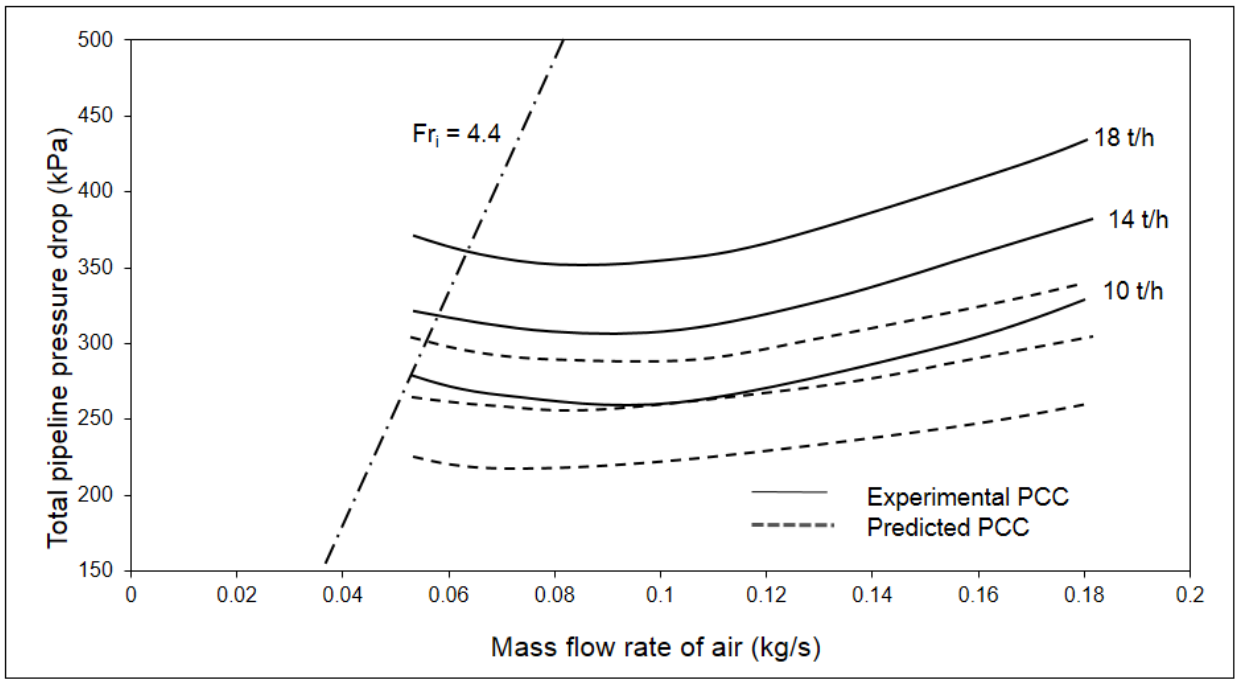

Figure 4.9. Experimental versus predicted PCC curve using unified two layer model and concept of equivalent length, FA2 through 65 mm I.D. × 254 m long pipe

Cement

Similar, concept was used as mentioned in the ESP dust. The cement was transported through same pipeline in which Fly ash (FA2) was transported. The results (see in figure 4.10) are in good agreement for both dense phase and dilute phase (slightly under predict at lower mass flow rate of air and slightly over predict at higher mass flow rate of air). Predicted PCC curves show gradual change in pressure drop at each mass flow rate of solids whereas the pressure drop of experimental curves show sharp increase from dense to dilute phase. The non-suspension term of two layer model for this material are showing slight changing in pressure drop at higher mass flow rate of air.

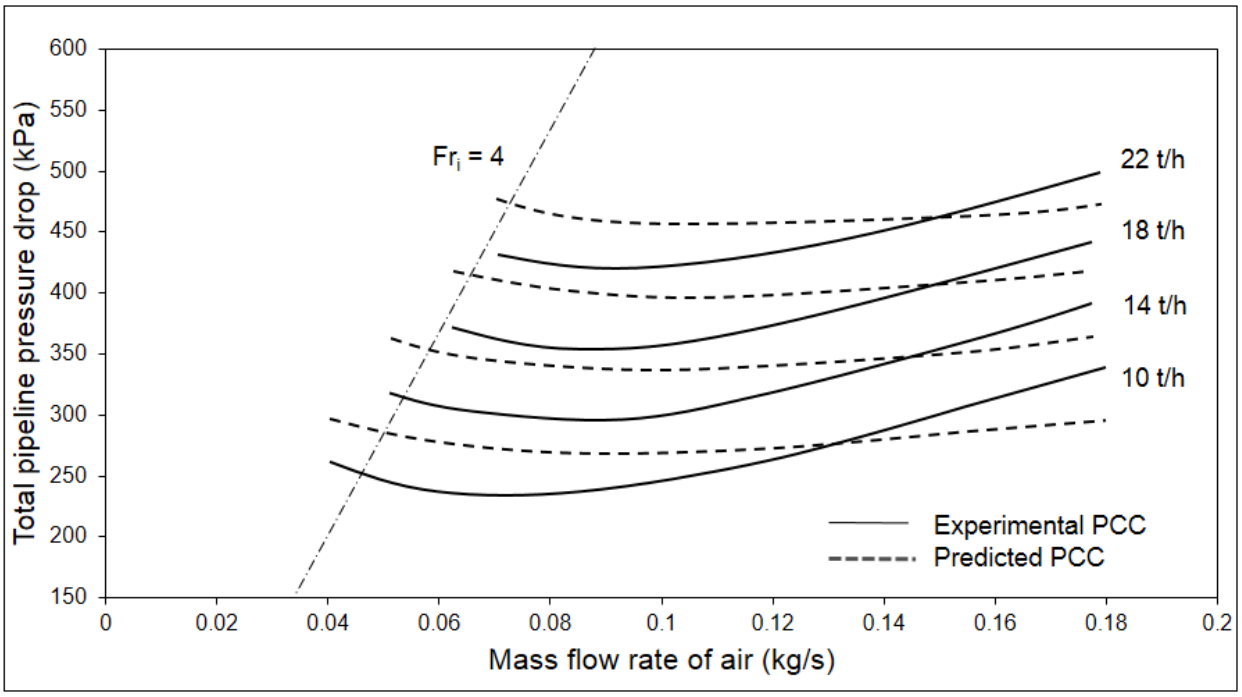

Figure 4.10. Experimental versus predicted PCC curve using unified two layer model and concept of equivalent length, cement through 65 mm I.D. × 254 m long pipe

The developed correlation of constants (i.e K, a,b and λ_s^*) of two –layer solid friction model are also validated on the other fly ash FA3 (ρ_b =634 kg/m^3; ρ_s =2197 kg/m^3; d_{50} = 15.5 µm; d_{10}=4.5 µm; d_{90} = 60 µm) in different pipelines and they are as follows. It was found that the results are well predicted in the range of delta (δ) from 1.48 to 1.52. The 'delta' is the function of particle size distribution and density ratio i.e. ratio of bulk density to the particle density. The amount of fine particles is directly proportional to the bulk density (William 2008). The bulk density and particle size distribution (PSD) are increased with increase of fine particles (d_{10}). however if the particle size distribution (PSD) is higher, then the value of δ will be more and the exponent of volumetric loading ratio would be highly negative, which leads to the instability and high inaccuracy in the model, similarly the lower particle size distribution (PSD) decrease the value of delta from its range and it provides negligible value of solids friction factor due to highly positive of exponent of volumetric loading ratio.

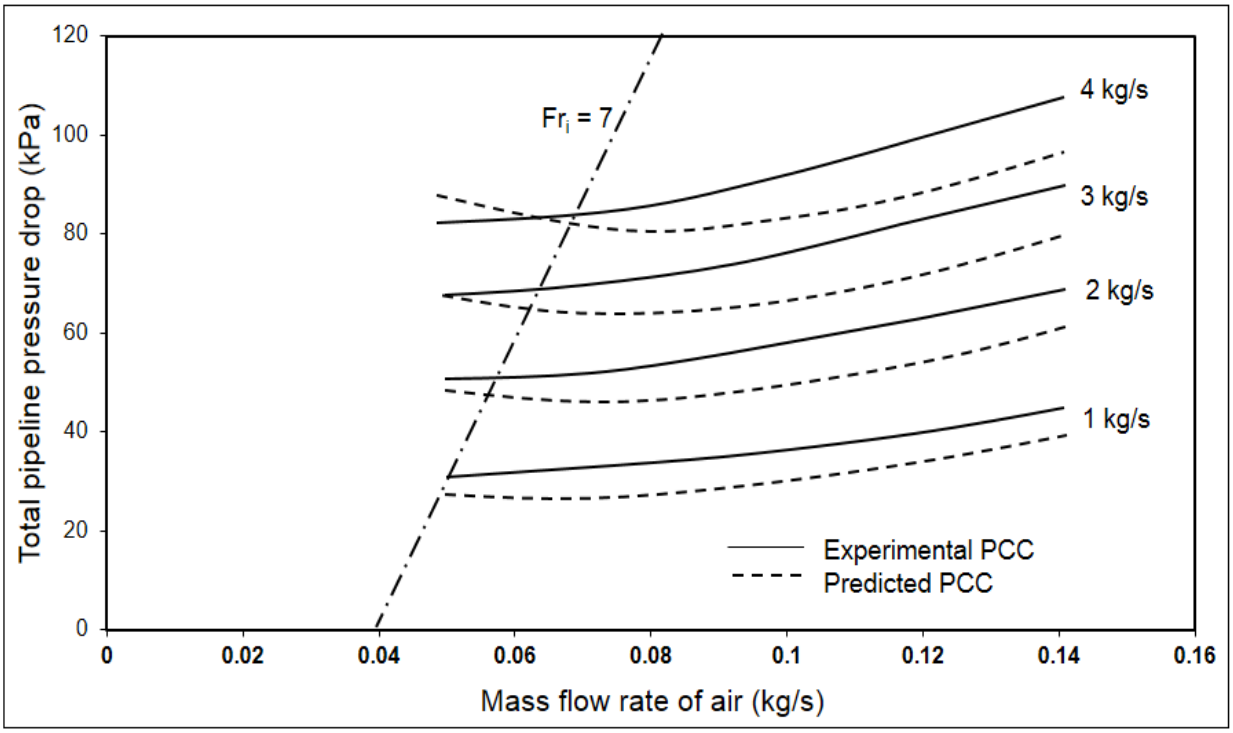

Figure 4.11. Experimental versus predicted PCC curve using unified two layer model and concept of equivalent length, fly ash through 80.5mm I.D. × 128.9 m long pipe.

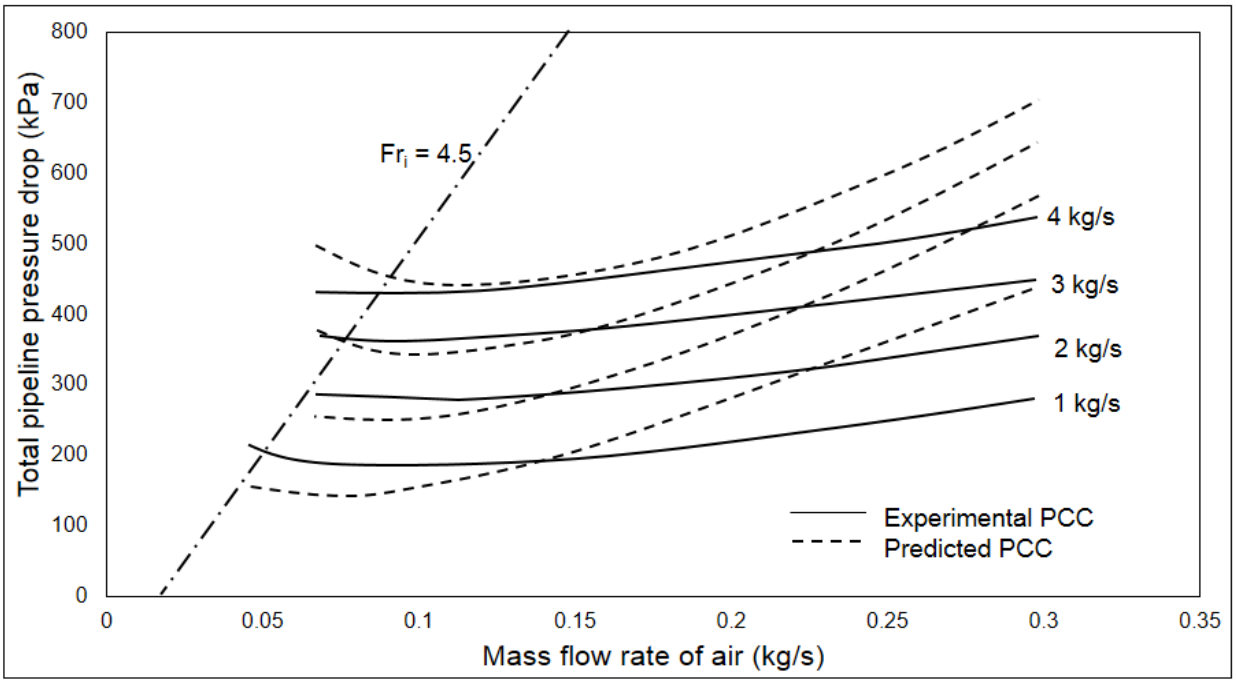

Figure 4.12. Experimental versus predicted PCC curve using unified two layer model and concept of equivalent length, fly ash through 69 mm I.D. × 546.7 m long pipe.

Figure 4.11 and 4.12 show the comparison of experimental and predicted pneumatic conveying characteristic curves of total pipeline pressure drop at different mass flow rate of solids. The derivation of constants (derived previously) was used to determine the value constants of two layer solid friction model for fly ash (FA3). The results for short pipeline in figure 4.11 is well predicted at both lower and higher mass flow rate of air. In the long pipeline, it gives good prediction near the minimum pressure drop in figure 4.12 and then suddenly after pressure minimum point the slope of predicted PCC curves increases sharply and deviates from experimental PCC.

Some keys points of unified two layer solid friction model

1. The value of constants provide accurate and stable results in the range of δ from 1.48 to 1.52. Actually the particle size distribution of developed two layer solid friction model for different materials was in a very small range.
2. The fine powders are available in very broad and narrow size distribution. However it is very difficult to predict the solids friction factor because of the range limitation of unified two layer solid friction model.
3. To overcome these limitations, the new friction factor model has been developed in the next chapter by considering products of different size distribution.

4.2 Modelling of solid friction model

4.2.1. Introduction

It was found in the previous section that the unified two layer model is applicable in a very short range of 'δ'. However there are lot of products at higher and lower particle size distribution (PSD) deviating from the defined range of 'δ'. In this section the new model format is developed for straight horizontal pipeline. The data has been used to determine the constants for new developed format and a unified model is introduced. After that it is validated with the experimental data.

Total pipeline pressure drop is the sum of pressure losses in horizontal, vertical and bend section. The pressure losses are mainly due to the particle-wall, particle-gas and particle-particle interaction and due to turbulence. It is important to determine accurate prediction of total pipeline pressure drop for different materials in various application. The over estimation of total pipeline pressure drop leads to wear in the pipeline attributing to excessive conveying velocity and more energy consumption while the under prediction of total pipeline pressure would cause decrease in the flow

rate of materials. Barth (1958) proposed the pressure drop equation (2.1) for gas –solids flow by considering the solids and air losses separately. This equation was originally developed to determine the pressure drop of coarse particles in dilute phase. Most of previous researchers (Pan and Wypych (1998), Stegmair (1978), Jones and Williams (2003), Setia and Mallick (2016)) have subsequently used this equation to determine the pressure drop for fine powders such as fly ash, ESP dust, transported in fluidized dense phase.

4.2.2. Development of Solid friction model

The challenging task in equation (2.1) is to determine the solids friction factor accurately. Solids friction factor is the term that combines the losses due to solid-solid interaction, solid-wall interaction, and solid –gas interaction. While lot of fundamental technique have been developed for coarse particle in slug flow, however it is very difficult to understand fundamental behavior of fine powders in higher mass loading ratio. In the literature one thing is commonly observed by several researchers, that smaller particles suppressed the turbulence while high inertial particle enhanced the turbulence. The researchers used various dimensionless terms such as Stoke number and particle diameter to create boundary between modulations of turbulence. In general pneumatic conveying flow, the material of different size particles is transported at higher mass loading ratio. The main difficulties in understand fundamental behavior of gas-solid interaction are mentioned by Mallick (2009) i.e. the nature of flow is quite complex so it is not easy to model the relevant particle and wall interactions and mechanisms; it is very difficult to derive the particle-particle interaction, particle wall interaction, particle air interaction and turbulence with the particle and bulk properties to model actual operating conditions. Owing to the complexity in understanding the fundamentals of flow mechanism, the researchers, such as (Rizk (1982), Wypych (1989), Pan (1992), Pan and Wypych (1998), Jones and Williams (2003), Mallick (2009). Setia and Mallick (2016)) preferred the empirical power based modelling to determine solid friction.

Previous literature in chapter (2) suggests that various models have been developed with different dimensionless terms such as Froude number, mass loading ratio, volumetric loading ratio, particle Reynolds number etc. to determine the solids friction factor of different materials by various researchers (Weber, Pan and Wypych (1998), Stegmair (1978), Jones and Williams (2003), Setia and Mallick(2016)). But these developed models have common limitations such as material specific i.e. the models have been developed only for particular material, while it shows the high

margin of error on other researcher's data for same or different material; there is no such model that can be applied for different fine powders and various pipelines to accurately determine the solids friction factor. In this chapter an attempt has been made to develop unified models for fine powders.

Procedure

1. To collect the total pipeline pressure drop data of various researchers, "Data from graphs" tool was used to extract data from researchers' thesis. The Authors and their experimental materials are as follows.

Table.4.2: Researchers and their experimental data

Researchers	**Materials**
Wypych (1989)	Pulverized coal and different fly ash
Pan (1992)	Pulverized brown coal and fly ash
Mallick (2009)	ESP dust , fly ash and white powder
Setia (2016)	Cement and fly ash

2. For scaling-up with system approach, Wypych and Arnold (1987) included adjustment factor for vertical length and bend losses. It was suggested that the equivalent length for vertical was twice the vertical length and 4 meter as per bend in line. While, Mills (2004) suggested equivalent length for vertical was same as previous mentioned by Wypych and Arnold (1987), however bend loss was compensated by bend loss data of conveying barites for other products and bend geometries. Mallick (2009) evaluated both concept for predicting pressure by system approach in fluidized dense phase flow of fly ash. The results were found grossly under-prediction.

The concept of equivalent length have been included to simplify the vertical length and bend loss in component approach in the present study.

$$L_e = L_H + 2L_v + 4N_b$$

Horizontal length, added to twice the vertical length and four times the number of bends gives the expression for equivalent length of total pipeline.

Table.4.3: Materials properties and pipe specification

Materials	Properties			L (m)	L_H (m)	L_V (m)	D (m)	Bends N × Radius(m) ×angle
	d_{50} µm	ρ_s kg/m3	ρ_b kg/m3					
Pulversied Coal	30	1600	760	25	21.4	3.6	0.052	5 ×1 × 90
Eraring fly ash	19.6	2350	500	71	67.4	3.6		11×1 × 90° And 2 ×90° blinded tee bends
Tallawarra fly ash	27.4	2160	880					
Munmorah fly ash	25.4	2100	650					
Vales point fly ash	18.8	2130	700					
Gladstone fly ash	17.6	2250	1030					
Wallerwang fly ash	11.5	2195	455					
Liddell fly ash	13.3	2415	640					
Fly ash (FA3)	15.5	2197	634	101.9	93.5	8.4	0.0525	8×0.254 × 90
				134.9	126.5	8.4	0.0525	8×0.254 × 90
				137.3	128.9	8.4	0.0805	8×0.254 × 90
				172	165.4	6.65	0.069	5×1 × 90
				553	546.7	6.3	0.069	17×1 × 90
Pulversied brown Coal	25.8	1488	437	172	165.4	6.65	0.069	5×1 × 90
				553	546.7	6.3	0.069	17×1 × 90
Cement (China)	19	2910	1080	254	237.9	16.1	0.065	10
Fly ash (FA2)	22	2370	660	254	237.9	16.1	0.065	10

ESP dust	7	3637	610	168	161	7	0.069	5×1 × 90 and one 154mm tee bend
				168	161	7	0.105	5×1 × 90 and one 154mm tee bend
				554	547	7	0.069	17×1 × 90
Fly ash (FA1)	30	2300	700	168	161	7	0.069	5×1 × 90 and one 154mm tee bend
				168	161	7	0.105	5×1 × 90 and one 154mm tee bend
				554	547	7	0.069	17×1 × 90

3. From the works of previous researchers, it was seen that solids friction factor depends on velocity, diameter of pipe, particle diameter, suspension density, particle density, viscosity of fluid/gas and particle size distribution.

$$\lambda_s = f\left(V, D, \rho_{sus}, g, d_{50}, \frac{d_{50}}{d_{90}-d_{10}}, \eta\right)$$

Particle size distribution $\left(\frac{d_{50}}{d_{90}-d_{10}}\right)$ represents the relationship between the median particle size and maximum variation between the size of solids.

BUCKHINGAM Pi THEOREM as explained in Cengel et al. (2003) is used for developing the model. The variables considered (n) in our problem have following dimensions:

η $[ML^{-1}T^{-1}]$

ρ_{sus} $[ML^{-3}T^{0}]$

d_{50} $[M^{0}L^{1}T^{0}]$

D $[M^{0}L^{1}T^{0}]$

$\frac{d_{50}}{d_{90}-d_{10}}$ $[M^{0}L^{0}T^{0}]$

V $[M^{0}L^{1}T^{-1}]$

g $[M^0L^1T^{-2}]$

As per three primary dimensions (m), the repeating variable selected are:

- Density (ρ_{sus})
- Diameter (D)
- Viscosity of fluid (η)

Remaining are primary variables as follows:

Particle diameter (d_{50})

Velocity of fluid (V)

Particle size distribution ($\frac{d_{50}}{d_{90}-d_{10}}$)

Gravity (g)

The number of л terms comes out to be four by using n-m. These are derived as follows

First Л term

$Л_1 = V_m a1\ \rho_{sus}^{b1}\ D^{c1} g$

$$Л_1 = \frac{V}{\sqrt{g\ D}} = Fr_g \quad (4.13)$$

Second Л term

$Л_2 = V_m^{a2}\ \rho_{sus}^{b2}\ D^{c2}\ (\frac{d_{50}}{d_{90}-d_{10}})$

$$Л_2 = (\frac{d_{50}}{d_{90}-d_{10}}) \quad (4.14)$$

Third Л term

$Л_3 = V_m^{a3}\ \rho_{sus}^{b3}\ D^{c3}\ \eta$

$$Л_3 = \frac{V\ D\ \rho sus}{\eta} \quad (4.15)$$

Fourth Л term

$Л_4 = V_m^{a4}\ \rho_{sus}^{b4}\ D^{c4}\ d_{50}$

$$Л_4 = \frac{D}{d_{50}} \quad (4.16)$$

From the above, the 3rd and 4th terms are combined to form a new term:

$$Л_3 / Л_4 = \frac{Vm\ d_{50}\rho sus}{\eta} = Re_{sd} \quad (4.17)$$

After solving the Pi/dimensionless term, the terms are modelled as:

$$\lambda_S = K\left(\frac{d_{50}}{d_{90}-d_{10}}\right)^a (\mathrm{Frg})^b\ (Re_{Sd})^c \quad (4.18)$$

4. The values of K, a, b, c are determined through regression method that was applied on above researcher's data by using Microsoft Excel software.

$$\lambda_S = 0.72\left(\frac{d_{50}}{d_{90}-d_{10}}\right)^{(0.43)} (\mathrm{Frg})^{-0.92}\ (Re_{Sd})^{-0.21}, \quad R^2 = 0.8999 \quad (4.19)$$

Newly developed model for solids friction factor, consists of three dimensionless terms which are particle size distribution, Froude number and modified Reynolds number (the suspension density is used instead of particle or fluid density). Here, Froude number represents the relationship of kinetic forces by mean fluid velocity, with the gravitational force included pipe diameter and Reynolds number shows relationship of inertial forces of gas solid mixture, with the viscosity of fluid. The exponents a, b, c and K are determined from the various products that were transported in the various pipelines (i.e. the different diameter and length) by previous researchers. The high value of exponent of the particle size distribution (eq. 4.19) suggests that the consideration of this parameter was required for unified modelling which was missing in the conventional models. The Froude number with the mean velocity and pipe diameter is the single most important parameter that can define the transition of dilute to fluidized dense phase in different pipeline for various products. The Froude number is maximum in the dilute phase flow, it decreases as the mean velocity of fluid decreases, so it is minimum in the dense phase flow. In the literature, it has been concluded that the smaller particles are inseparable from the fluid. They follow the fluid fluctuation due to their low inertia, hence it dampens the turbulence due to dissipative forces such as drag forces, crossing trajectories etc. So, the suspension density was introduced considering the combined effect of gas solids mixture. While Ratnayaka (2007), has used the suspension density instead of fluid density in the modified Darcy Weisbach equation and then modelled the friction factor for gas-solid mixture with the entry velocity of fluid.

4.2.3 Scale-up validation of unified model

In this section, the newly developed unified model for solids friction factor using the steady state conveying data of various products, and in different pipelines has been evaluated to check their accuracy and stability by using the total pipeline pressure drop of experimental data and various data of other researchers. The bend and vertical losses have been compensated with the concept of equivalent length. The percentage error in pressure drop for different materials conveyed in various pipeline are shown in the following table. The positive sign of percentage error represents that the pressure drop has been under predicted, whereas the negative sign shows that the predicted pressure drop is more than the actual pressure drop (i.e. over prediction). The percentage of error lies between +20 to -20 percentage for most of the materials in various pipelines. Whereas fly ash (FA3) is showing over prediction in smaller and shorter pipelines, however same material in longer pipeline reduces the percentage error.

After that an attempt was made to reduce the percentage error by correlating the percentage error with particle /bulk properties such as bulk density, particle density, particle size distribution fluidization velocity etc. But it is not possible taking into account only the materials properties because the percentage error also depends on the mass flow rate of air and mass flow rate of solids in same pipeline for same products. The percentage error also depends on the geometric properties of pipeline such as length and diameter. Extensive experimental investigation is required to take into account all these factors to provide a criteria for calculating the error and hence minimize it.

Table 4.4: Percentage error of total pipeline pressure drop of different material in various pipeline

Materials	L (m)	L_H (m)	L_V (m)	D (m)	Percentage error $\left(\frac{\Delta P_{actual} - \Delta P_{predicted}}{\Delta P_{actual}}\right)\times 100$	
					Maximum	Minimum
Pulversied Coal	25	21.4	3.6	0.052	22	-2
Eraring fly ash	71	67.4	3.6		25	9
Tallawarra fly ash					-23	-9
Munmorah fly ash					-14	3
Vales point fly ash					16	-2
Gladstone fly ash					14	-2
Wallerwang fly ash					22	-20
Liddell fly ash					25	20
Fly ash (FA3)	101.9	93.5	8.4	0.0525	-50	-4
	134.9	126.5	8.4	0.0525	-50	7
	137.3	128.9	8.4	0.0805	-20	-10
	172	165.4	6.65	0.069	-20	10
	553	546.7	6.3	0.069	-24	10
Pulversied brown Coal	172	165.4	6.65	0.069	25	-11
	553	546.7	6.3	0.069	-19	0.45
Cement (China)	254	237.9	16.1	0.065	23	4
Fly ash	254	237.9	16.1	0.065	25	6
ESP dust	168	161	7	0.069	30	0.2
	168	161	7	0.105	20	-18
	554	547	7	0.069	25	6
Fly ash	168	161	7	0.069	5	-20
	168	161	7	0.105	-40	-11
	554	547	7	0.069	-40	-18

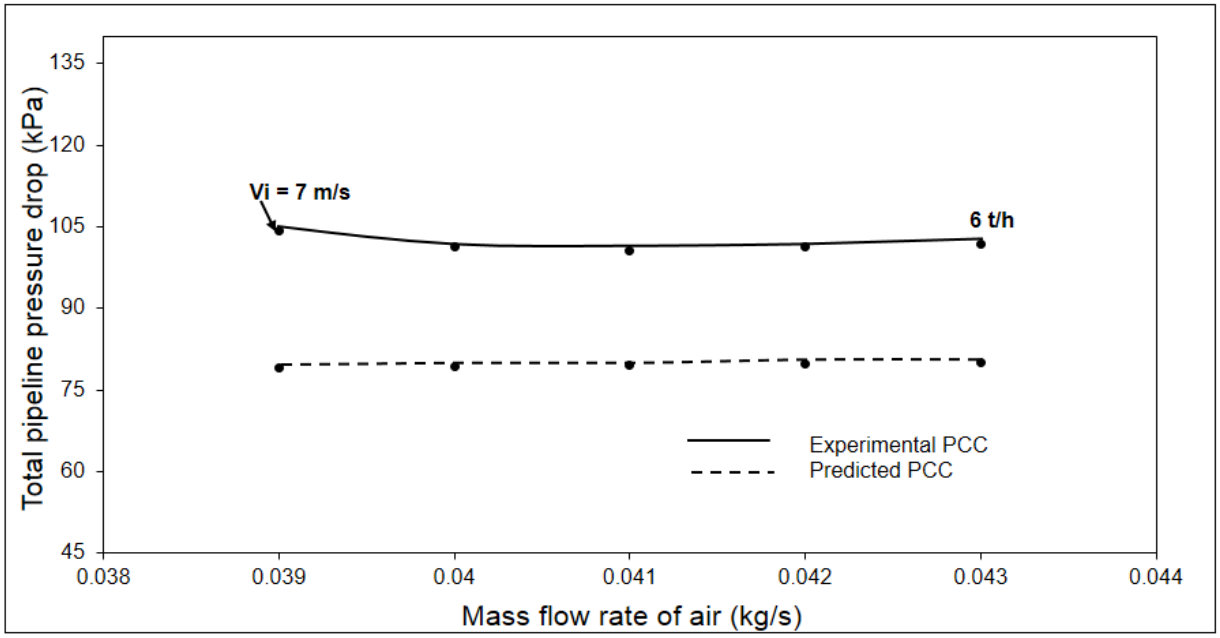

Figure 4.13. Experimental versus predicted PCC curve using newly developed model and concept of equivalent length, white cement through 54 mm I.D. × 70 m long pipe with 6 t/h mass flow rate of solid.

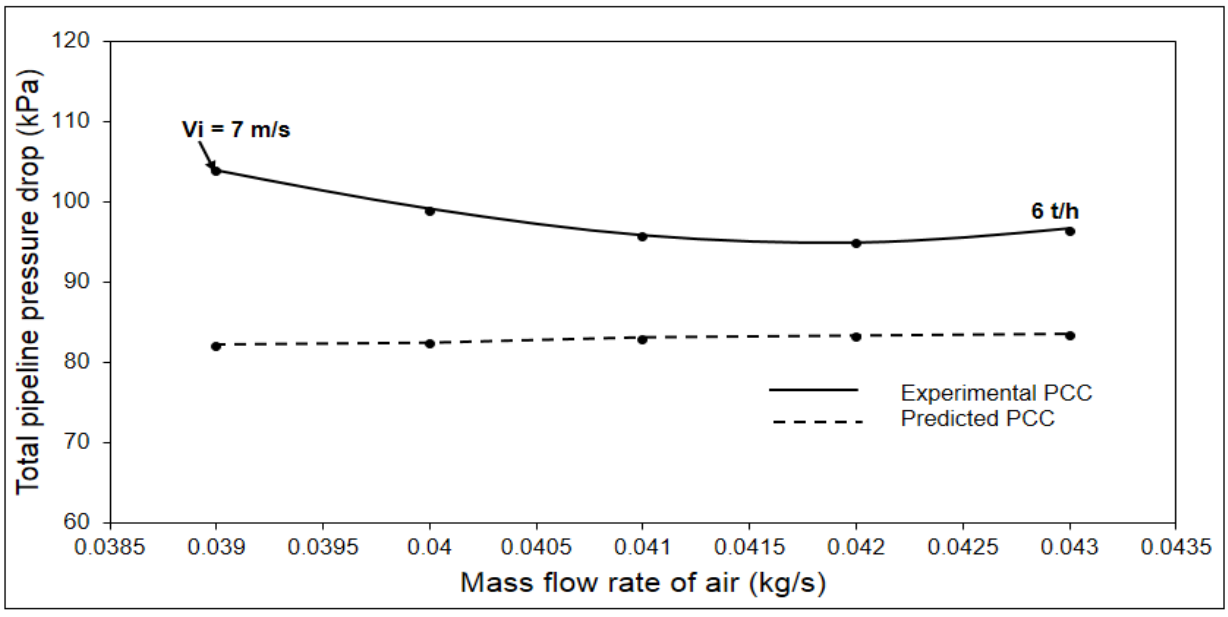

Figure 4.14. Experimental versus predicted PCC curve using newly developed model and concept of equivalent length, grey cement through 54 mm I.D. × 70 m long pipe with 6 t/h mass flow rate of solid.

Figures 4.13 and 4.14 show total pipeline pressure drop of experimental and predicted pneumatic conveying characteristic curves. It shows that both white and grey cement have been transported at 7 m/s inlet conveying velocity and the predicted pressure drop for both figures gives an under prediction at 6 t/h mass flow rate of solids. Possible causes of under prediction can be the concept of equivalent lengths. The pressure drop through bend may be more than 4 meter straight horizontal pipeline. The high frequency vibration in the vertical pipe was observed during transporting the products. Thus it increases the turbulence in the pipeline, hence the pressure drop of vertical length can be more than it was considered in the concept of equivalent length. The trend of pneumatic conveying characteristic curve show less variation of pressure drop in grey cement because of negligible change in mass flow rate of conveying air, whereas the trend of pneumatic conveying characteristic curve in white cement initially varies the pressure drop by changing the mass flow rate of air but then almost pressure remain constant. The trend of predicted curve shows increase in pressure drop from lesser mass flow rate of air to higher and hence deviation of predicted curve from experimental curve is decreasing as mass flow rate of air increases in grey cement. However, the deviation of pressure drop of predicted and experimental curve also reduces in white cement but rate of decreasing deviation is very slow.

Chapter 5

Evaluation of pressure minimum curve

5.1 Introduction

In this chapter a relation has been developed to determine the pressure minimum curves for different fine powders. The pressure minimum curve is the locus of minimum pressure drop points for different values of solids flow rate, and provides the optimal and reliable conveying conditions for a given product. Generally if the mass flow rate of air lies on the right hand side of the curve, then flow is categorized as dilute phase, whereas if it lies on the left hand side of the curve then it is categorized as dense phase flow, which leads to deposition of solids in pipe bottom (Ratnayake (2005)). Rose and Duckworth (1969) carried out the experiments to develop the minimum conveying velocity expression by transporting the mustard seed, lead bead, glass bead and steel bead through 32 mm pipeline. The following expression is provided for minimum conveying velocity for dilute phase.

$$V_{min} = 2.33\, G_s^{0.286}\, D^{0.5}\, d^{-0.857}\, \rho_p^{-1}\, \rho^{0.714}\, U_t^{1.43} \qquad (5.1)$$

Rizk (1982) conducted the experiments to determine the minimum conveying velocity by using two test materials (Styropor and Polystyrol) conveying through 50 to 400 mm diameter pipeline. The expression for minimum conveying velocity is presented as:

$$m^* = (1/10^{\delta}) \times Fr_i^{\chi} \qquad (5.2)$$

Where $\delta = 1.44\, d + 1.96$ and $\chi = 1.1d + 2.5$

Weber (1981) provided the expressions for minimum conveying velocity in equation, however, did not clearly indicate whether these expressions represent both dense and dilute phase flow.

For $U_t \leq 3$m/s $\qquad Fr_i = [(8/3)\, U_t + 7]\, m^{*0.25}\, (d_p/D)^{0.1} \qquad (5.3)$

For $U_t \geq 3$m/s $\qquad Fr_i = 15\, m^{*0.25}\, (d_p/D)^{0.1}$

Kalman et al. (2005) conducted experiment by conveying glass, zirconium, alumina, iron, salt sand, talk and ammonium oxide and developed a pickup velocity model (equations 5.4 to 5.5) using a modified Reynolds number (Re_p*) and Archimedes number term.

For Ar> 16.5 $Re_p^* = 5\ Ar^{(3/7)}$ (5.4)

Where, Ar represents the Archimedes number and Re_p^* represents the Reynolds number modified by pipe diameter.

For 0.45 <Ar< 16.5 $Re_p^* = 16.7$ (5.5)

For Ar< 4.5 $Re_p^* = 21.8\ Ar^{(1/3)}$

Bansal (2012) evaluated these models for fine powders. The results showed that the models were providing distinct location of pressure minimum curve away from actual pressure minimum curve. The reason of distinct location may be: a) Because the majority of these models are developed to determine the minimum conveying velocity for coarse materials; b) The transition phenomenon from dense to dilute is different for fine and coarse products, there is gradual change for fine powders as compared to coarser material where the change is more sudden. Bansal (2012) also provided a new model to determine the pressure minimum curve for fine powders. The correlation was developed for fine fly ash (particle density: 2300 kg/m^3, bulk density: 700 kg/m^3 and d_{50} :30 μm) and white powder (particle density: 1600 kg/m^3, bulk density: 620 kg/m^3 and d_{50}: 55 μm) is presented as:

For Fly ash, $Re_p = 8.027\ Ar^{1.001}$ (5.6)

For White powder, $Re_p = 1.694\ Ar^{1.004}$ (5.7)

These provided models are only for fly ash and white powder in straight pipeline conveying. The value of minimum velocity obtained for total pipeline pressure drop of given products was on a location different from experimental value in pneumatic conveying characteristic curve.

The literature survey describes that the previous researchers used particle diameter, particle/fluid density ratio, mass loading ratio, pipe diameter etc. to determine the minimum conveying velocity. However, a unified relation to determine the minimum velocity for fine powders was still not developed. In the physics of gas-solid interaction, Hadinoto (2005) distinguishes between responsive and unresponsive particles with Stoke number. The author represents higher inertia

particles with Stoke number greater than 0.1 which indicates the enhancement of turbulence, whereas the lower inertial particles denoted by Stoke number less than 0.1 indicating suppressed intensity of turbulence. The Stoke number is defined as the ratio of particle relaxation time (ability of particles to adjust to new conditions) to the characteristic eddy turnover time. This is the single parameter that accounts for the particle, geometric and fluid properties and with the help of it one is able to differentiate between the higher and lower inertia particles. The following pneumatic conveying characteristic curves are drawn with the constant Stoke number line near the minimum conveying velocity.

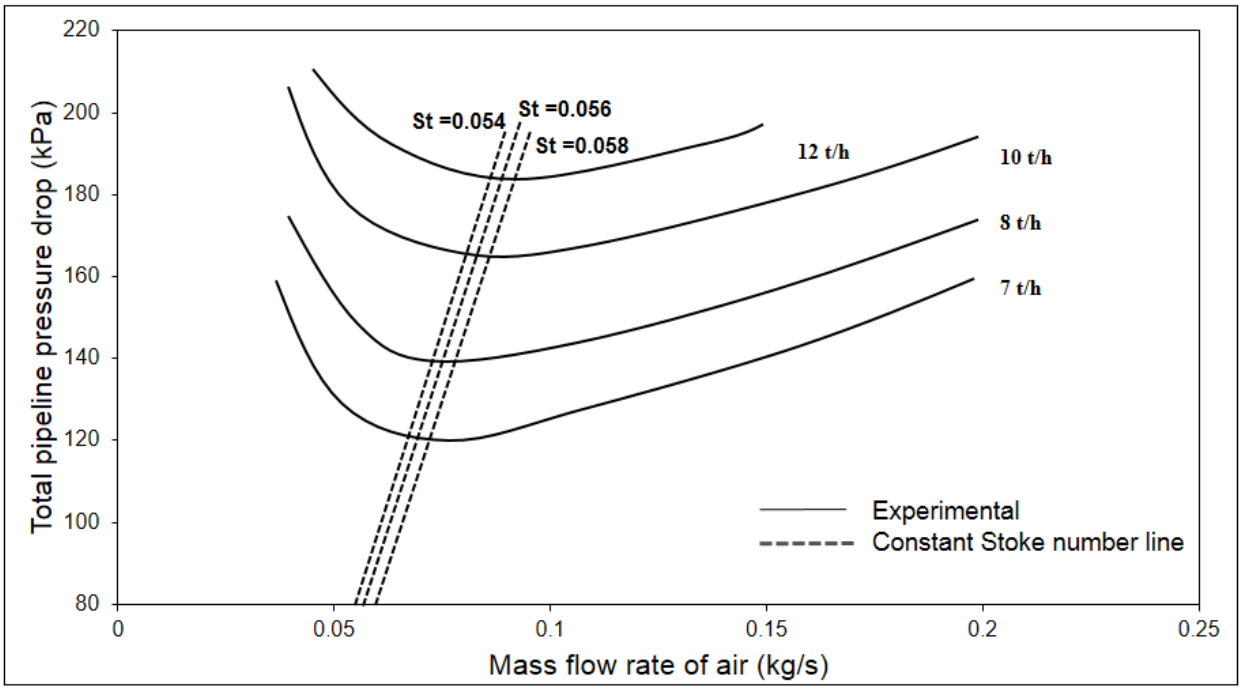

Figure 5.1. Experimental PCC curves with the constant Stoke number line, ESP dust through 69 mm I.D. ×168 m long pipe with different mass flow rate of solid.

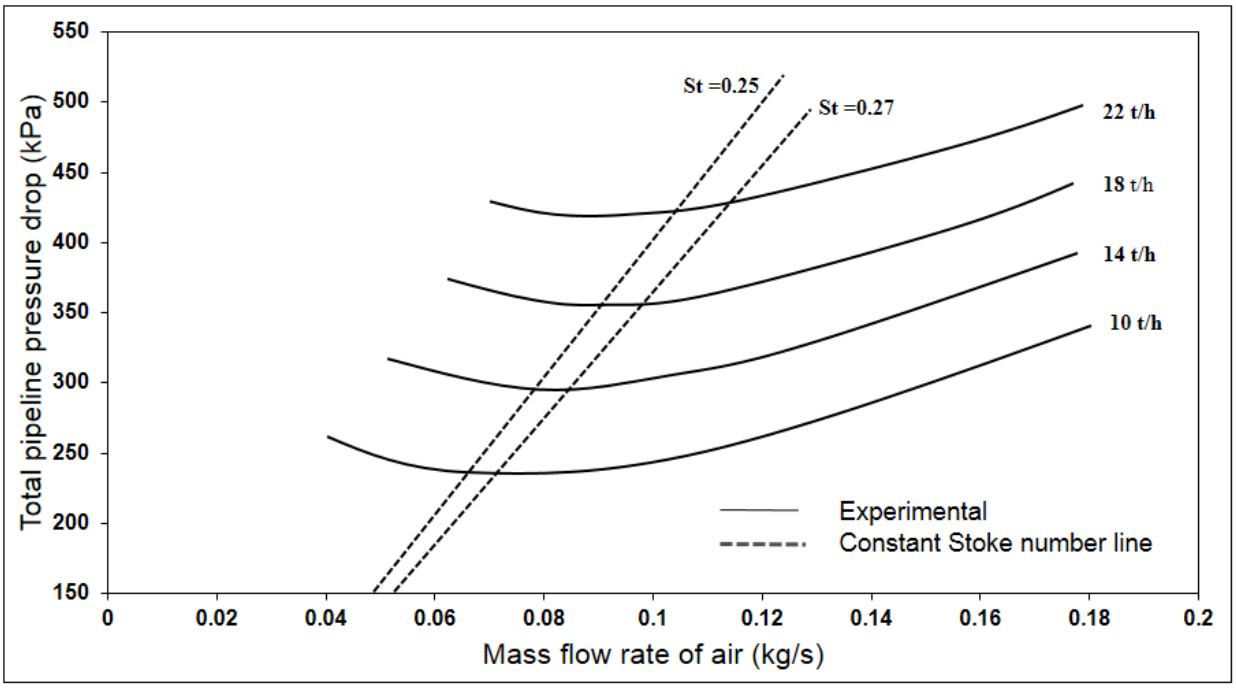

Figure 5.2. Experimental PCC curves with the constant Stoke number line cement through 65 mm I.D. × 254 m long pipe with different mass flow rate of solid.

The figures 5.1 and 5.2 show the experimental conveying characteristic curves for ESP dust and cement respectively. These figures also show the range of Stokes number at which the minimum conveying velocity lies for different mass flow rates of solids. The particle size of ESP dust is small as compared to that of cement due to which the Stoke number for ESP dust is less than that of cement.

The contribution of Stokes number and ratio of particle diameter to the length scale of the most energetic eddy are accounted for at the pressure minimum points to determine the minimum conveying velocity by analyzing the given products in different pipeline. The relation of integral length scale of eddy with the radius of pipe was defined by conveying gases at different Reynolds number by (Hutchinson (1971)). The following correlations have been defined for fine powders.

$St^a \times (d_p/l_e)^b = K_1$

Where $St = \frac{V_i \rho_p {d_p}^2}{18\mu D}$

$l_e/R \approx 0.2$

$l_e/D \approx 0.1$

$l_e = 0.1D$

When the data was analyzed it was found that the value of constant 'a' in the above equation is 0.4 and value of constant 'b' is 0.6. Hence it provides a range of values for the constant 'K_1'. It approximately lies between 75 and 85.

$$St^a \times (d_p/0.1D)^b = K_1 \quad 5.8$$

$$St^{0.4} \times (d_p/0.1D)^{-0.6} \approx 18.8 \text{ to } 21.35 \quad 5.9$$

$$St^{0.4} \times (d_p/D)^{-0.6} \approx 75 \text{ to } 85 \quad 5.10$$

Table 5.1. Percentage error of predicted minimum velocity for different products.

Product	Pipeline Configuration	Stoke number range at minimum pressure drop	d_p/l_e	K_1	Error (%) $(V_{min.A} - V_{min.P})/(V_{min.A})\times100$
ESP dust	69 mm I.D. ×169 m	0.053-0.058	1.01×10^{-3}	80	5
ESP dust	105 mm I.D. ×169 m	0.035-0.040	6.67×10^{-4}	80	-15
ESP dust	69 mm I.D. ×554 m	0.052-0.056	1.01×10^{-3}	80	8
Fly ash (FA1)	69 mm I.D. ×169 m	0.43-0.48	4.35×10^{-3}	80	15
Fly ash (FA1)	105 mm I.D. ×169 m	0.36-0.42	2.85×10^{-3}	80	-25
Fly ash (FA1)	69 mm I.D. ×554 m	0.38-0.42	4.35×10^{-3}	80	25
Cement	65 mm I.D. ×254 m	0.25-0.27	2.92×10^{-3}	80	15
Fly ash (FA2)	65 mm I.D. ×254 m	0.28-0.32	3.38×10^{-3}	80	10

The above table shows the percentage error between the experimental and predicted values of minimum conveying velocity. The minimum conveying velocity falls where the value of constant

K lies between 75 and 85. The value of constant K is considered as 80 for all given products. The percentage error with negative sign represents that the predicted velocity is toward the dilute phase whereas positive percentage error shows the actual velocity is greater than the predicted velocity, it means the predicted velocity shows the pressure minimum curve toward the dense phase as compared to actual pressure minimum curve. The maximum error is observed for larger pipeline of fly ash. This may be attributed to the integral length scale of eddy which was determined by assuming single phase of flow. In reality however, the flow is two phase. Other possible cause of deviation in actual and predicted value and consideration the value of K equal to '80' is the geometric configuration of different pipeline. It means the different size of bends at different location along the pipeline and also the number of bends vary for each pipeline.

Chapter 6

Conclusion and Future scope

6.1 Conclusion

In this study, an attempt was made to create a unified solids friction factor model. First, the two layer solids friction factor model of different materials that was given by Setia (2016) was considered. The constants for different materials of two layer model were derived with the material properties such as particle size distribution, bulk density, particle density, terminal velocity and particle Froude number. The results obtained predict fairly well pressure drops in total pipeline at both higher and lower mass flow rate of air. The concept of equivalent length has been used to compensate for the bend and vertical length loss in total pipeline pressure drop. The FA1 and ESP dust through longer pipe under predicted the values of pressure drop in dense phase flow. Through larger pipe, in the case of ESP dust predicted pressure drop values are very similar to experimental data but in the case of FA1 there is a greater margin of error. The slopes of predicted PCC curves of FA2 is quite similar to experimental data. Cement provided good results for both dense and dilute phase. The obtained pneumatic conveying characteristic curve are providing fairly well prediction near the pressure minimum curve in given products. But the applicability of this model was very limited in the the range of 'δ' from 1.48 to 1.52. The delta 'δ' of fly ash (FA3) lies in given range. So the results are predicted well for both shorter and longer pipeline.

Secondly, considering the wide range of fine products, new unified model was developed with the group of three dimensionless terms. It was validated with the total pipeline pressure drop of experimental data. The predicted values give a fairly accurate prediction (14 to 23% degree of under prediction). It has been observed that the equivalent lengths do not address losses for bend and vertical length properly. An attempt was made to reduce the error by correlating error with the material properties such as particle/bulk density, fluidization velocity, particle size and size distribution. However, it could not be carried out successfully because the error depends on a large number of parameters and extensive experimental work needs to be done to include each of the varying factors.

Also, a relation was found for fine powders to determine the pressure minimum curve as follows:

$$St^{0.4} \times (d_p/D)^{-0.6} \approx 80 \quad 6.1$$

The error between experimental and predicted values of minimum conveying velocity was found to lie between -15 to 15 percent except for larger and longer pipelines of fly ash (FA1).

This empirical work would help designer in reliable and optimal designing of pneumatic conveying system.

6.2 Future scope

Although unified model was developed for fine powders, but still the percentage error is higher. It was observed that in order to make a unified model for fine powders with minimum percentage error a lot of experimentation is required for a wide range of fine powders to understand the effect of each property on the pressure drop.

References

Bansal, A. 2012. ME Dissertation: Investigation into straight pipe pressure drop and flow-mode transition criteria for fludised dense-phase pneumatic conveying systems, Thapar University.

Barth, W. 1958. Strömungsvorgänge beim transport von festteilchen und flüssigkeitsteilchen in gasen. Chemie – Ing. – Techn. 30 (3): 171-180.

Behera, N., Agarwal, V. K., Jones, M. G. and Williams, K. C. 2013a. CFD modeling and analysis of dense phase pneumatic conveying of fine particles including particle size distribution. Powder Technology, 244, 30-37.

Behera, N., Agarwal, V. K., Jones, M. G. and Williams, K. C. 2013b. Modeling and analysis for fluidized dense phase conveying including particle size distribution. Powder Technology, 235, 386-394.

Datta, B.K. and Ratnayaka, C. 2003. A simple technique for scaling up pneumatic conveying systems. Particulate Science and Technology. 21: 227-236.

Datta, B.K. and Ratnayaka, C. 2005. A possible scaling-up technique for dense phase pneumatic conveying. Particulate Science and Technology. 23: 201-204.

Elgobashi, S. 1994. On predicting particle laden turbulent flows. Applied Scientific Research. 52: 309-329.

Gore, R.A. and Crowe, C.T., 1989. Effect of particle size on modulating turbulent intensity. International Journal of Multiphase Flow, 15(2), pp.279-285.

Hetsroni, G., 1989. Particles-turbulence interaction. International Journal of Multiphase Flow, 15(5), pp.735-746.

Hadinoto, K. and Curtis, J.S., 2009. Reynolds number dependence of gas-phase turbulence in particle-laden flows: Effects of particle inertia and particle loading. Powder Technology, 195(2), pp.119-127.

Hadinoto, K., Jones, E.N., Yurteri, C. and Curtis, J.S., 2005. Reynolds number dependence of gas-phase turbulence in gas–particle flows. International journal of multiphase flow, 31(4), pp.416-434.

Jones, M.G. and Williams, K.C. 2003. Solids friction factors for fluidized dense phase conveying. Particulate Science and Technology. 21: 45-56.

Kalman H., Satern, A. Meir, D. and Rabinovich E. 2005. Pickup (critical) velocities of particles, Powder Technology, Vol. 160: 103-113.

Klinzing, G.E. and Rizk F., Marcus R.D., Leung L.S. 2010. Pneumatic conveying of solids - A theoretical and practical approach. Third edition. Springer.

Mallick, S.S. 2009. PhD Dissertation: Modelling dense-phase pneumatic conveying of powders, University of Wollongong.

Mallick, S.S. and Wypych, P.W. 2009. Minimum transport boundaries for pneumatic conveying of powders. Powder Technology. 194: 181-186.

Mallick, S.S., Wypych, P.W. and Pan, R. 2011. Minimum Transport Boundaries for Dense-Phase Pneumatic Conveying of Powders. In the proceedings of Bulk Solids India, Mumbai.

Mills, D. 2004. Pneumatic conveying design guide. Elsevier/Butterworth-Heinemann, 2nd edition.

Pan, R. 1992. PhD Dissertation: Improving scale-up procedures for the design of pneumatic conveying systems, University of Wollongong.

Pan, R. and Wypych, P.W. 1992. Scale up procedures for pneumatic conveying design. Powder Handling and Processing. 4 (2): 167-172.

Ratnayake C. 2005. PhD Dissertation: A Comprehensive Scaling Up Technique for Pneumatic Transport Systems, Norwegian University of Sceince and Technology (NTNU).

Rizk, F. 1982. Pneumatic transport in dilute and dense phase. Bulk Solids Handling. 2 (2): 235-241.

Setia, G., Mallick, S. S., Wypych, P. W. and Pan, R. 2013. Validated scale-up procedure to predict blockage condition for fluidized dense-phase pneumatic conveying systems. Particuology, 11, 657-663.

Setia, G., Mallick, S.S., Pan, R. and Wypych, P.W., 2016. Modeling solids friction factor for fluidized dense-phase pneumatic transport of powders using two layer flow theory. Powder Technology, 294, pp.80-92.

Stegmaier, W. 1978. Zur berechnung der horinentalen pneumatischen forderung feinkorniger feststoffe - for the calculation of horizontal pneumatic conveying of fine grained solids. Fordern and Heben. 28: 363-366.

Weber, M. 1981. Principles of hydraulic and pneumatic conveying on pipes. Bulk Solids Handling. 1 (1): 57-63.

Weber, M. 1991. Friction of the air and the air/solid mixture in pneumatic conveying. Bulk Solids Handling. 11 (1): 99-102.

Williams, K.C.2008. Phd Dissertation: Dense phase pneumatic conveying of powders, University of Newcastle.

Williams, K.C. and Jones, M.G. 2004. Numerical model velocity profile of fluidised dense phase pneumatic conveying. In the proceedings of 8th International Conference on Bulk Materials Storage and Transportation, Wollongong, NSW, Australia, 5-8 July: 354-358.

Wirth, K.E. and Molerus, O. 1983. Prediction of pressure drop with pneumatic conveying of solids in horizontal pipes. Journal of Powder and Bulk Solids Technology. 7 (2): 17-20

Wypych, P. W. 1989. PhD Dissertation: Pneumatic conveying of bulk solids, University of Wollongong.

Wypych, P.W and Yi, J. 2003. Minimum transport boundary for horizontal dense-phase pneumatic conveying of granular materials. Powder Technology. 129: 111-121.

Wypych, P.W. and Arnold, P.C. 1987. On improving scale-up procedures for pneumatic conveying design. Powder Technology. 50: 281-294.

Appendices

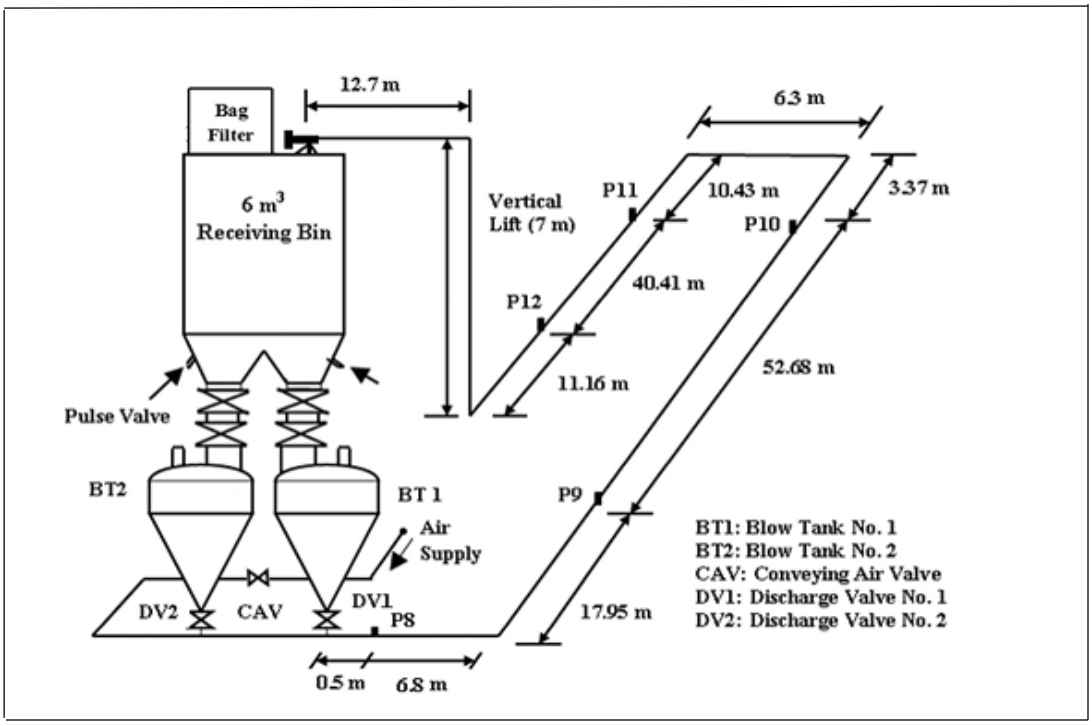

Figure A1: layout of the 69 mm I.D. × 168 m test rig at the University of Wollongong, Australia

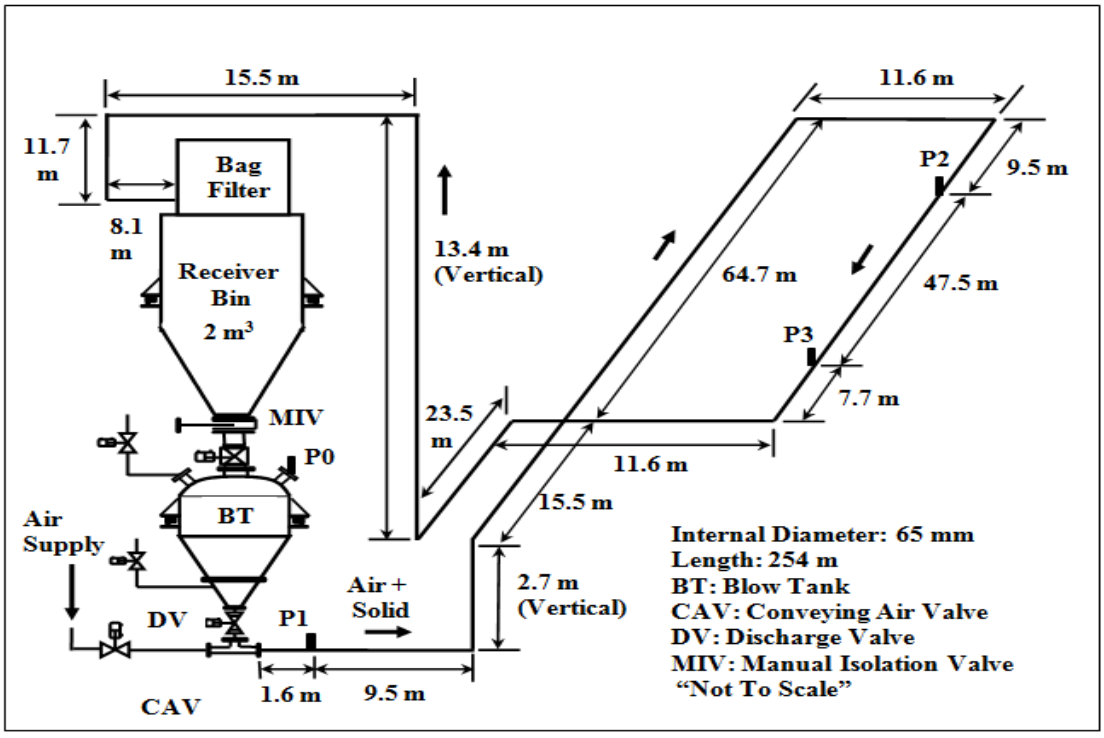

Figure A2. Layout of the 65 mm I.D. × 254 m test rig at Fujian Longking Co., Ltd., China